



**UNIVERSITY „POLITEHNICA” of BUCHAREST
DOCTORAL SCHOOL OF AEROSPACE ENGINEERING**

SUMMARY OF THE PH.D. THESIS

Optimal solutions for small launchers

Author: Eng. Alexandru-Iulian ONEL

Ph.D. supervisor: Prof. dr. eng. Teodor-Viorel CHELARU

DOCTORAL COMMITTEE

President	R.S.I dr. eng. Teodor Lucian GRIGORIE	from	University POLITEHNICA of Bucharest
Ph.D. supervisor	Prof. dr. eng. Teodor-Viorel CHELARU	from	University POLITEHNICA of Bucharest
Reviewer	R.S.I dr. eng. Mircea CERNAT	from	Romanian Space Agency
Reviewer	Lect. dr. eng. Ciprian-Marius LARCO	from	Military Technical Academy “Ferdinand I”
Reviewer	Lect. dr. eng. Laurențiu Eugen MORARU	from	University POLITEHNICA of Bucharest

**BUCHAREST
2021**

Contents

1	Introduction	4
1.1	Thesis overview	4
1.2	Context.....	4
1.3	Objectives	5
1.4	Current state of research	5
2	Overview of the multidisciplinary optimization algorithm.....	6
3	Study on the weights and sizing assessment	7
3.1	Overview	7
3.2	Mathematical modelling	7
3.2.1	Upper Structure	7
3.2.2	Lower structure	8
3.3	Validation of the model	9
4	Study on the propulsive performance assessment.....	10
4.1	Overview	10
4.2	Mathematical modelling.....	10
4.3	Validation of the model	11
5	Study on the aerodynamic characteristics assessment	12
5.1	Overview	12
5.2	Breakdown schemes	12
5.3	Mathematical modelling.....	12
5.4	Validation of the model	14
6	Study on the launcher dynamics and trajectory optimization	15
6.1	Overview	15
6.2	Reference frames	15
6.3	Coordinate transformations	15
6.4	Gravitational model	15
6.5	Dynamic models	15
6.5.1	Six degrees of freedom model – 6DOF.....	15
6.5.2	Three degrees of freedom model – 3DOF.....	16
6.6	Orbital parameters	17
6.7	Launcher evolution phases	17
6.8	Auxiliary data	17
6.9	Validation of the model	18

7	Additional details on the multidisciplinary optimization algorithm	19
7.1	Solution selection and advancement algorithm	19
7.2	Optimization variables	19
7.3	Requirements and input data	20
7.4	Objective function	20
8	Optimization of a nominal launcher constructive solution	22
8.1	Preliminary design requirements	22
8.2	Convergence of the developed algorithm	22
8.3	Constructive solution	23
8.4	Baseline trajectory	24
8.5	Mission validation	25
9	Parametric analysis regarding small launchers	26
9.1	Target orbit altitude impact	26
9.2	Payload mass impact	27
9.3	Typical missions impact	28
9.4	Used propellant impact	30
10	Conclusions	31
10.1	Thesis contributions	31
10.2	Results obtained	32
10.3	Prospects for future development	33
10.4	List of publications	34
	Bibliography (selective)	35

1 Introduction

The thesis summarizes a series of studies on the main aspects necessary for the preliminary design of small satellite launchers constructive solutions. Based on the studies performed, algorithms were developed for sizing the launcher, to determine its propulsive and aerodynamic characteristics, simulating the dynamics of motion and optimizing the trajectory. Four individual computational codes for the disciplinary analyses were developed, existing mathematical models being extended or completed with own formulations. At the same time, a multidisciplinary optimization algorithm (MDO) capable of generating preliminary constructive solutions specific to small launchers was developed. The MDO algorithm, which incorporates the individual disciplinary analyses codes, generates launchers that are able to fulfil the imposed mission (to insert one or more satellites in a predefined orbit), the optimization of the launcher being realized by minimizing its lift-off mass.

Keywords: *multidisciplinary optimization, space launcher, propulsive performance, aerodynamic characteristics, trajectory optimization, orbital parameters, parametric analysis*

1.1 Thesis overview

The first chapter has an introductory character, presenting the current global context of small launchers, the objective of the thesis, and also the current state of research in the field. In the second chapter an overview of the developed MDO algorithm is realized, being presented the block scheme and listed the main modules (disciplinary analyses) and the secondary ones.

The next four chapters present the studies dedicated to the four main disciplines that are addressed, being presented the mathematical models necessary for the sizing process of the small launcher, estimating its propulsive and aerodynamic characteristics, but also for the development of two motion simulators. Chapter seven details the secondary modules used in the multidisciplinary optimization algorithm, presenting the solution selection and advancement algorithm, the components of the optimization variables vector, the formulation used to define the objective function, the design requirements and the input data.

In the eighth chapter, the MDO algorithm developed in the thesis is used for the optimization of the nominal small launcher, corresponding to a baseline mission. Both the launcher and the reference trajectory to be followed to maximize its orbital insertion performance are detailed. Chapter nine presents a parametric analysis, structured in four independent studies, on the influence of the main design requirements on the minimum mass launcher configuration. The influence of target orbit altitude, payload mass, typical missions and the type of propellant (oxidizer - fuel pair) used on the launcher characteristics is quantified.

In the tenth chapter, the thesis contributions are highlighted, the conclusions of the thesis are detailed, the perspectives of further development are presented and the scientific papers published during the elaboration of the thesis are listed.

1.2 Context

This section presents the current context, favorable to the development of small launchers, the main observations being:

- Increasingly resources are allocated to space programs (development of satellites and launch vehicles);
- Launchers dedicated for small satellites (reduced dimensions and mass) represent a niche in the fleet of launch vehicles currently on the market;

- The typical missions of small satellites are those of terrestrial observation in different spectra (target orbits are those of low altitude and high inclination);
- Due to the miniaturization of components and systems, there is a constantly growing market for compact satellites in the mass range 100 kg – 250 kg, which attracts an increased demand for small launchers dedicated to them;
- The use of liquid propellant rocket engines is preferred due to its high performance and long operating time;
- The use of launchers with a low number of stages (two-stage architecture) is preferred due to their low complexity and increased reliability.

1.3 Objectives

The thesis presents in detail the main aspects necessary for the development of a small satellite launcher preliminary constructive solution. The main objective of the thesis is to develop a computational code (multidisciplinary optimization algorithm) capable of generating optimal solutions for small launchers according to design requirements, including imposed orbital performance. For the development of this algorithm, the existing mathematical models in the literature have been extended or completed with own formulations.

1.4 Current state of research

At present, in the Romanian technical literature, there are no papers that address the topic of small launcher optimization. Externally, the studies published in the field are limited, often using a simplified approach, which consists in using components already on the market or in an advanced stage of research, optimizing only the architecture of the launcher [1]. The thesis aims at a detailed approach, consisting in both generating the architecture and optimizing all major launcher subsystems. Obtaining the optimal solution for a launcher is a process of great difficulty due to the numerous disciplines that must be addressed. Thus, the optimization of a launcher, even of small dimensions, is in fact a multidisciplinary optimization process, being performed both at the assembly/subassembly level and at the global level.

Summarizing the study dedicated to the current state of research (*State of the art*), possible implementation methods within the multidisciplinary optimization code are the following:

- AAO (All At Once), used in [2] for the preliminary design of a reusable stage and in [3] for the optimization of a spacecraft trajectory;
- IDF (Individual Discipline Feasible), used in [4] to minimize complex mathematical functions and in [5] for the preliminary design of a supersonic plane;
- MDF (Multi Discipline Feasible), used in [6] to optimize an re-entry trajectory into the atmosphere, in [7] to define an orbital insertion maneuver, in [8] to optimize a liquid propellant rocket engine and in [9] to optimize an ascending trajectory.

Theoretically, at convergence, all 3 methods allow the generation of constructive solutions (launchers) that are technically feasible. At the convergence of the AAO method, the internal residue function is close to zero, but may not be null. At the convergence of the IDF method, the obtained architecture may include internal coupling functions that are not fully respected. Thus, the launcher obtained may be technically incorrectly defined at the assembly or subassembly level. Because for each iteration of the multidisciplinary optimization iterative process, when using a MDF method, the solution corresponds to a technically feasible configuration [10], this method is the most flexible, being the one implemented in the MDO code developed in the thesis.

2 Overview of the multidisciplinary optimization algorithm

In order to obtain the optimal solution for the small launcher design it is necessary to use a complex multidisciplinary optimization process (MDO). In addition to the preliminary design of the launcher, the mission profile is also optimized, imposing a reference trajectory to follow. The block scheme of the developed MDO algorithm is presented in Fig. 2.1.

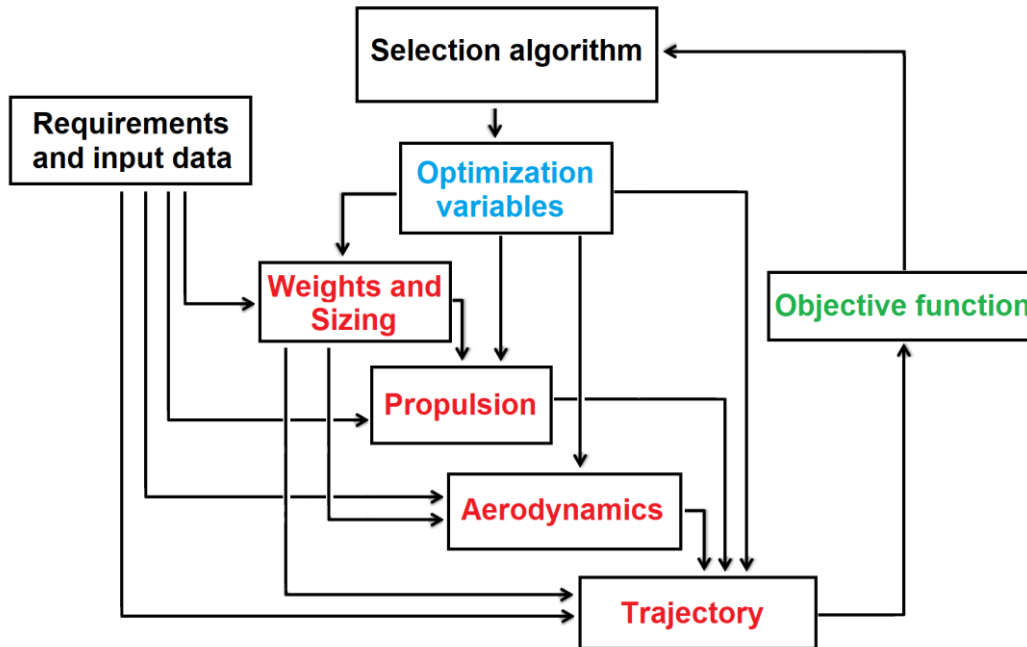


Fig. 2.1 Block scheme of developed MDO algorithm

The small launcher optimization is done by obtaining an optimization variables vector, following the use of a solution selection and advancement algorithm based on the objective function evaluation. The solution is considered optimal at the convergence of the MDO algorithm, when the objective function has not improved after a specified number of iterations.

The choice of optimization variables is made in accordance with the launcher requirements and its architecture. The launcher is then completely defined through them and the global input data using the mathematical models integrated inside the main MDO blocks/modules. The disciplinary analyses are done in a cascade sequence, the core of the program being made up of the following 4 main modules: *Weights and Sizing*, *Propulsion*, *Aerodynamics* and *Trajectory*.

In the *Weights and Sizing* module, the launcher is sized both at a global level and at a major assemblies and subassemblies level. At the same time, its mass breakdown is being realized. The *Propulsion* module determines the propulsive performance of liquid propellant engines. Within the *Aerodynamics* module, the aerodynamic characteristics of interest of the symmetrical axial launcher are determined. In the *Trajectory* module, the launcher motion is analyzed. The motion simulator is based on a simplified dynamic model (3DOF), the developed computational code being in addition capable of optimizing the ascending trajectory of the launcher.

The mathematical models used for each of the main modules are independent of another, thus in total 4 individual codes are developed, which, after validation, are incorporated in the multidisciplinary optimization code. Along with the 4 main modules listed above, within the architecture of the multidisciplinary optimization algorithm, there are also the following secondary modules: *Requirements and input data*; *Optimization variables*; *Objective function*; *Selection algorithm*.

3 Study on the weights and sizing assessment

3.1 Overview

The first study is dedicated to the weights and sizing assessment of the launcher, mathematical models being developed for estimating its external dimensions, its mass breakdown, but also its preliminary interior planning. The mathematical models detailed in this chapter are necessary for the first main module of the MDO algorithm (according to Fig. 2.1). The *Weights and Sizing* module implements a bottom-up approach, the dimensions and masses of the launcher components being individually calculated. As depicted in Fig. 3.1, this ensures that in the end, by summing the individual contributions, one can determine the dimensions and mass of each stage, the upper structure, and then of the entire n -stage launcher. The launcher breakdown scheme is valid for both sizing and weights assessment.

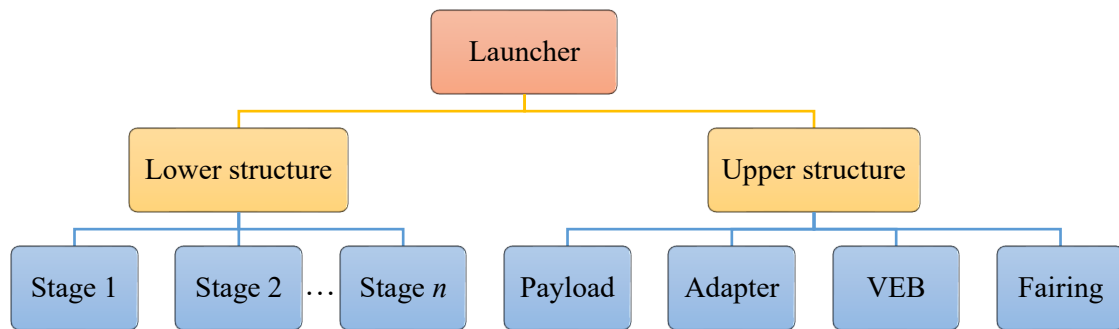


Fig. 3.1 Launcher weights and sizing breakdown scheme

3.2 Mathematical modelling

The mathematical model used for the weights and sizing assessment of the launcher, in the context of an iterative MDO process, must be: robust, so that it can be used regardless of the optimization variables selected by the solution advancement algorithm; fast, so as not to require a long computational time; precise, so that the resulting data correspond to a correct estimate of the architecture, size and mass of the launcher constructive solution. For these reasons, analytical and semi-empirical models are preferred.

3.2.1 Upper Structure

The upper structure, in the case of a small launcher, consists of: Payload, in the form of one or numerous satellites; Satellite adapter; Vehicle Equipment Bay (VEB), which houses the avionics and additional electrical systems required for the mission; Fairing, which protects the satellite from outer conditions. The mass and dimensions of each of these components must be estimated in order to be integrated into the architecture of the launcher.

Component mathematical modelling is done as follows:

- Payload – input data;
- Adapter – semi-empirical model [11];
- VEB – semi-empirical model [12];
- Fairing – semi-empirical model developed based on own results and those of [11], in which the fairing mass (measured in kg) is:

$$M_{fairing} = 7.12 \cdot S_{lateral} \quad (3.1)$$

with $S_{lateral}$ is the fairing lateral surface area (measured in m^2).

A clear representation of the upper structure component breakdown is shown in Fig. 3.2.

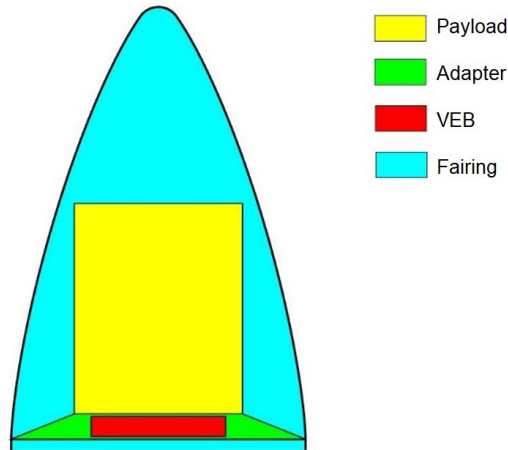


Fig. 3.2 Upper structure breakdown

3.2.2 Lower structure

For the lower structure modelling, the masses and dimensions of each stage are calculated individually, their contributions being latter summed up. For stages which incorporate a liquid propellant engine, the breakdown scheme implemented is shown in Fig. 3.3, a visual representation of the main components (and interior planning) being observed in Fig. 3.4.

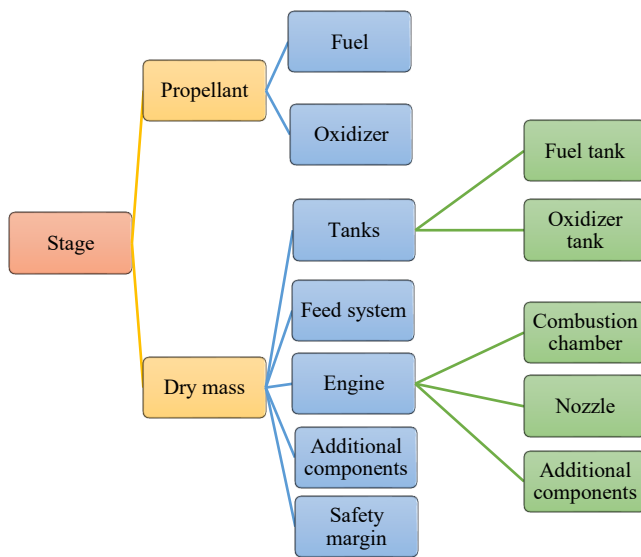


Fig. 3.3 Stage breakdown scheme (liquid propellant engine)

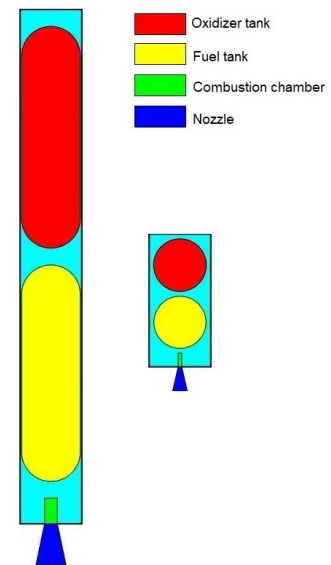


Fig. 3.4 Stage main components

Component mathematical modelling is done as follows:

- Propellant – optimization variable;
- Oxidizer and fuel – based on the mixture ratio (details in chapter 4);
- Tanks – analytical models [12], [13], [14];
- Feed system: mechanical turbopumps – semi-empirical models [13], [14];
- Combustion chamber – semi-empirical model [13], [14];
- Nozzle – analytical model [13];
- Engine – semi-empirical model [13], [14];
- Additional components – semi-empirical model [13];
- Safety margin: length - 10% ; dry mass - 5%.

A dry mass safety margin of 5% and a length safety margin of 10% are also implemented to boost the overall confidence of the MDO assessment (can be lowered or set to 0 in the detailed phase of launcher design).

3.3 Validation of the model

To validate the mathematical models implemented in the *Weights and Sizing* module, a total of 8 stages were used, for which reference data could be gathered, the data analyzed being the stage dry mass and length. In order to demonstrate the flexibility of the developed model, both small and medium-large stages were studied. The estimation errors for these 8 stages can be found in Table 3.1, the average error following the comparisons being about 5.8%. For a better visualization of the differences between the reference values and those obtained with the developed model, the structural mass of the stage is presented in Fig. 3.5.

Table 3.1 Developed model estimation error

Launcher	Stage	Dry mass error [%]	Length error [%]	Average error [%]
Atlas V	Atlas CCB	2.61	0.83	1.72
Atlas V	Centaur	11.01	4.81	7.91
Ariane 5, G	EPC H158	6.31	7.67	6.99
Ariane 5, ES	EPC E/H173	5.99	1.18	3.58
Ariane 4	H10-3	8.24	0.81	4.52
Delta III	DCSS	2.82	13.18	8.00
Delta IV	DCSS, 4m	0.70	8.61	4.65
Delta IV	DCSS, 5m	11.46	6.35	8.91
All stages		6.14	5.43	5.79

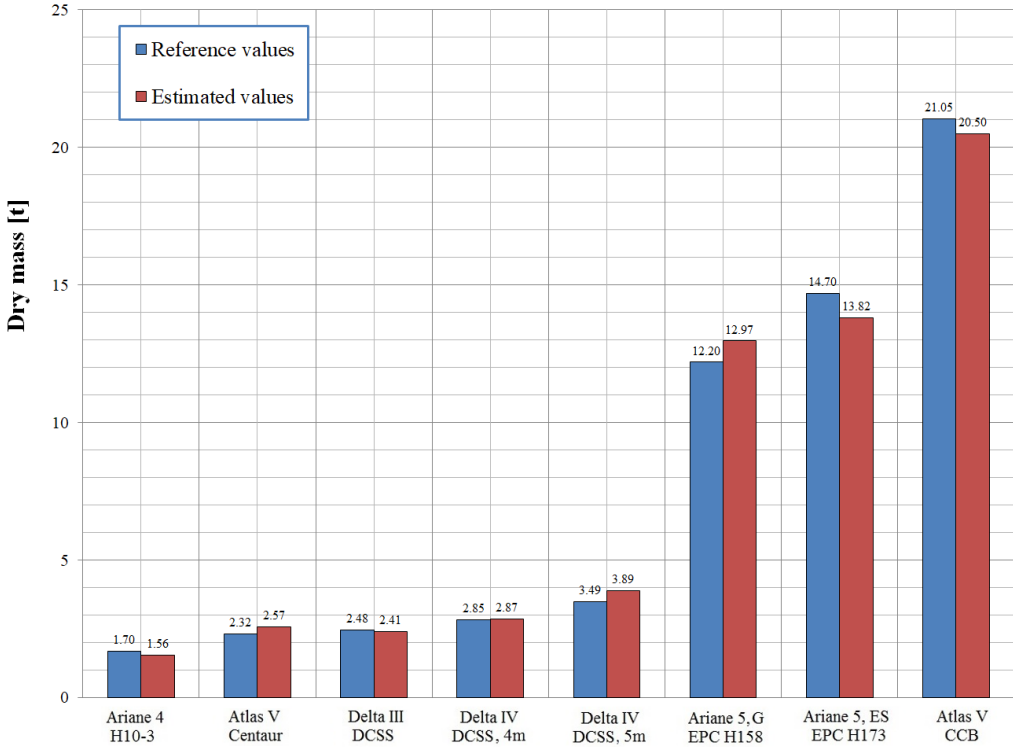


Fig. 3.5 Weights estimation

4 Study on the propulsive performance assessment

4.1 Overview

The second study is dedicated to the estimation of propulsive performances of liquid propellant rocket engines, the developed mathematical models being necessary for the *Propulsion* module within the multidisciplinary optimization algorithm (according to Fig. 2.1). It is necessary to determine the thrust curves for each constituent stage of the launcher. The 4 most common pairs of liquid propellants (oxidizer/fuel) are studied: Oxygen/Kerosene; Oxygen/Methane; Oxygen/Hydrogen; Oxygen/Ethanol.

4.2 Mathematical modelling

Thrust (T) assessment uses the classical, analytical formulation:

$$T = q \cdot g_0 \cdot I_{sp} \quad (4.1)$$

where q is the propellant mass flow rate, g_0 is the standard gravitational acceleration, and I_{sp} is the specific impulse.

In order to determine the thrust it is necessary to estimate the specific impulse, together with the expansion ratio, the characteristic velocity of the exhaust gases and their gas constant. Summarizing the mathematical models detailed in the thesis, in order to obtain the propulsive characteristics of liquid propellant engines, it is necessary to estimate 4 propulsive parameters: the optimal oxidizer/fuel mixture ratio (R_m), the flame temperature (T_f), the relative gas molecular weight (M_w) and the gas specific heat ratio at the throat (γ).

The typical approach to obtain the four main propulsive parameters is by direct calling the classical combustion charts and interpolating its data [15]. This method is not practical in terms of required computational time in the context of an MDO algorithm (multiple calls). Thus, there is a need for a simpler model that does not require multidimensional data interpolation, in the thesis being developed nonlinear power functions using the following formulation:

$$f(x, y) = a + b \cdot x^c + d \cdot y^e \quad (4.2)$$

where $f = (R_m, T_f, M_w, \gamma)$, $x = P_c$ (combustion chamber pressure), $y = P_e$ (exhaust pressure), and (a, b, c, d, e) are the model coefficients.

Thus, 4 combustion surfaces (per pair of propellants) are generated, specific to each propulsive parameter of interest. The values of the (4.2) model coefficients were determined following a nonlinear regression analysis, using the TR (Trust-Region) [16] and LM (Levenberg-Marquardt) [17] algorithms. The developed model is valid for P_c values in the range of 10-250 atm and P_e values in the range of 0.1-1 atm. An example of the coefficients corresponding to the oxygen/kerosene pair is given in Table 4.1

Table 4.1 Oxygen/Kerosene approximation function coefficients

Function	Variable		Coefficient				
	x	y	a	b	c	d	e
R_m [-]	P_c [atm]	P_e [atm]	0.40488	1.80306	0.04244	-0.27005	0.07216
T_f [K]	P_c [atm]	R_m [-]	-96657.5664	100008.738	0.00111	-20471.89	-5.10454
M_w [-]	P_c [atm]	R_a [-]	-61.87059	35.50626	0.00568	39.03287	0.22586
γ [-]	P_c [atm]	R_a [-]	2.83175	-1.6644	0.00204	0.16136	-1.06601

4.3 Validation of the model

A total of 11 liquid propellant rocket engines were analyzed, with nominal thrust ranging from 30kN to 7.7MN. All four pairs of liquid propellants mentioned earlier were studied to validate the mathematical model, the data of interest being the specific impulse and thrust (at sea level and in vacuum). The results obtained with the developed mathematical model are presented in Table 4.2. The estimation errors are shown in Fig. 4.1.

Table 4.2 Developed model estimation errors

Engine	Reference values				Estimated values			
	I_{sp} [s] s.l.	I_{sp} [s] vac.	T [kN] s.l.	T [kN] vac.	I_{sp} [s] s.l.	I_{sp} [s] vac.	T [kN] s.l.	T [kN] vac.
Rocketdyne F-1	263	304	6770	7770	263.66	305.40	6665.14	7720.35
Merlin 1C-F9	263	302	409.24	469.29	265.56	303.63	420.59	480.88
Merlin 1D	282	320	654.33	742.41	273.49	311.87	634.57	723.62
Rocketdyne J-2	-	424	-	1023.09	-	420.74	-	993.23
Rocketdyne RS-25	366	452.3	1705.83	2090.66	362.25	439.25	1679.94	2037.04
JAXA 30 kN class	234	335	-	30	225.59	332.73	-	29.79
JAXA 100kN class	-	356	-	98	-	353.34	-	97.78
DLR SE-12	322.5	348.3	3844	4152	315.85	342.11	3764.72	4077.76
DLR L75	-	315	-	75	-	313.75	-	74.64
Glushko RD-101	214	240	363	402	221.04	246.02	374.79	417.14
Glushko RD-103	220	251	432	500	224.95	251.49	433.27	484.37

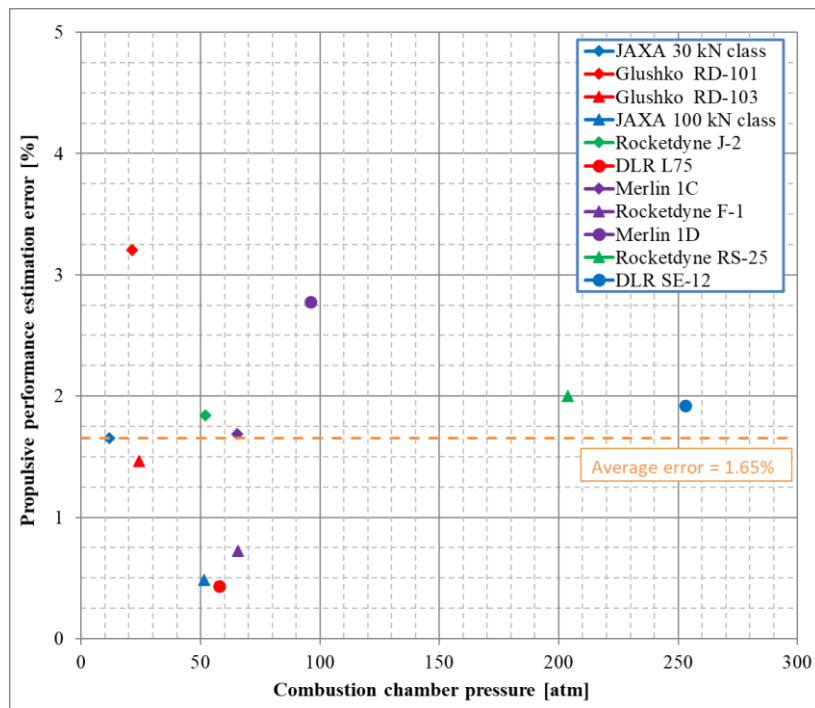


Fig. 4.1 Developed model accuracy vs. combustion chamber pressure

The mathematical model has a high degree of accuracy, the overall average error being about 1.65%. At the same time, using relations of type (4.2), the computational time is significantly reduced compared to the multidimensional interpolation of the combustion charts.

5 Study on the aerodynamic characteristics assessment

5.1 Overview

Following the study dedicated to the determination of aerodynamic characteristics, mathematical models were developed for the estimation of axial force coefficient (C_A), normal force coefficient (C_N), drag coefficient (C_D) and lift coefficient (C_L) for axisymmetric launch vehicle configurations. Analytical and semi-empirical methods have been used because of their high flexibility and low computational time needed. Considering the transformation relations between the body axis and wind axis systems, as well as the axial symmetry of the configuration, for the implemented 3DOF dynamic model (details in chapter 6) it is necessary to numerically generate only the aerodynamic databases:

$$C_D = f(\alpha, M); C_N = f(\alpha, M) \quad (5.1)$$

where α is the angle of attack, and M is the Mach number.

5.2 Breakdown schemes

A standard outer geometry does not exist for launchers, as they come in different shapes and sizes. Therefore, it is practical to breakdown the launcher into simple components from a geometric point of view. A small launcher can be seen as an assembly consisting of the following components: nose/tip/fairing (multiple geometries), cylindrical stages, positive transitions and negative transitions. A simple launcher can consist of only two components, a nose and a cylindrical stage. Complex launchers can include numerous cylindrical stages, but also transitions between them. The case of a complex generic launcher, having a 3-stage architecture that contains both types of transitions, is presented in Fig. 5.1, 2D and 3D representations being visible. For such a launcher, there are a total of 7 individual components.

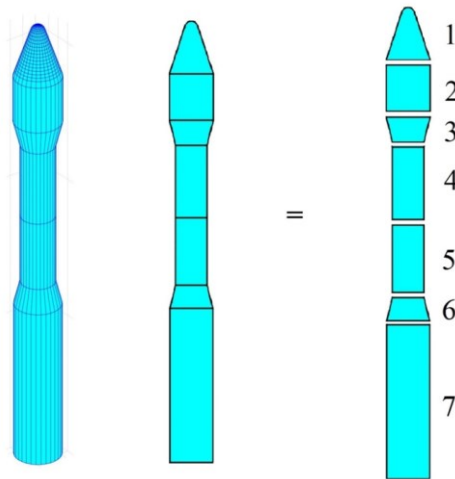


Fig. 5.1 Launcher breakdown into simple individual components

Most modern launchers do not use fins due to their inefficiency at low speeds, the vehicle stabilization being achieved through the high-performance control systems implemented (TVC + RCS). In the case of small launchers auxiliary boosters are not needed.

5.3 Mathematical modelling

For the drag coefficient evaluation, the following relation is used:

$$C_D(\alpha, M) = C_{d_0}(M) + C_{d_i}(\alpha) \quad (5.2)$$

where C_{d_0} is the zero angle of attack drag coefficient, and C_{d_i} is the alpha drag coefficient.

Different ways of decomposing the drag force (at null angle of attack) exists in the literature [18], in the thesis being used a breakdown into body pressure drag, friction drag and base drag.

For each individual i^{th} launcher component, its contribution to the zero angle of attack drag coefficient $C_{d_{0i}}$ is computed using:

$$C_{d_{0i}} = C_{d_{0body.pressure}} + C_{d_{0friction}} + C_{d_{0base}} \quad (5.3)$$

Summarizing the study presented in the thesis, mathematical modelling is done as follows:

- Body pressure drag coefficient $C_{d_{0body.pressure}}$ – analytical [19], [20] and semi-empirical models [21] for transition components and standard profiled noses (conical, ogive, Haack series). For blunted noses (with bluntness ratio G_r) a model using a correction factor $F_{c,r}$ applied to the standard $C_{d_{0body.pressure}}$ has been developed:

$$F_{c,r} = 1 - 0.16 \cdot G_r + 4.6 \cdot G_r^2 \quad (5.4)$$

- Base drag coefficient $C_{d_{0base}}$ – analytical [21] and semi-empirical models [22];
- Friction drag coefficient $C_{d_{0friction}}$ – analytical and semi-empirical models, dependent on the flow regime (laminar, transitional, turbulent) [23];
- Alpha drag coefficient C_{d_i} – semi-empirical models [24], [25].

For the normal force coefficient evaluation, a simple breakdown relation is used:

$$C_N = \sum_i^N (C_{N_i}) \quad (5.5)$$

where N is the number of individual simple geometric components, and for the calculation of the individual contributions C_{N_i} of all components the following linear formulation is used:

$$C_{N_i} = C_{N_{i\alpha}} \alpha \quad (5.6)$$

in which $C_{N_{i\alpha}}$ is computed using:

$$C_{N_{i\alpha}}(\alpha, M) = C_{N_{incomp_{i\alpha}}}(\alpha) \cdot F_{comp}(\alpha, M) \quad (5.7)$$

where $C_{N_{incomp_{i\alpha}}}$ is the incompressible normal force derivative, and F_{comp} is a compressibility factor.

The term $C_{N_{incomp_{i\alpha}}}$ is estimated using Barrowman model [23], together with the Galejs extension [26]. For the term F_{comp} , based on own results, CFD results from literature [27] and experimental data [28], [29], for cylindrical stage components, and non-conical noses, the following approximation was developed:

$$F_{comp} = p_1 + p_2 M_c + p_3 \alpha + p_4 M_c^2 + p_5 M_c \alpha + p_6 \alpha^2 \quad (5.8)$$

where α is the launcher angle of attack, measured in degrees, $M_c = M \sin \alpha$ is the crosswind Mach number, and the model coefficients $P = (p_1, \dots, p_6)$ are:

$$P = \begin{cases} (1, & 0.6973, 0.0155, 24.9025, -0.3652, -0.0056) & , \text{if } M \leq 0.8 \\ (1, & -0.0596, 0.0821, -1.0376, 0.2040, -0.0143) & , \text{if } M > 0.8 \end{cases} \quad (5.9)$$

For the other simple geometric components, hybrid models based on relation (5.8) and other similar formulations are developed in the thesis.

5.4 Validation of the model

To validate the developed mathematical model, a CFD campaign was employed for a test configuration (similar to the one in Fig. 5.1), in order to obtain a high-fidelity aerodynamic database. The CFD campaign matrix totaled a number of 72 cases, being divided into two sets. In the first set, a classical approach was used, in which the dissociation of air does not occur. This first set consists of: 18 cases with $\alpha = 0^\circ$, 18 cases with $\alpha = 4^\circ$ and 18 cases with $\alpha = 8^\circ$, with Mach numbers ranging from 0.01 to 10. Additionally, in the second set, 18 cases in which the species transport was activated for very high launcher velocities were performed. The Park model for dissociated air was used together with the related reaction model [30]. A FR/ED (finite rate/eddy dissipation) turbulence-chemistry interaction model was chosen. All CFD cases were performed using a $k-\omega$ SST turbulence model. The convective flux was calculated with the Roe-FDS scheme.

Summarizing the most important results presented in the thesis, one can see:

- The drag coefficient C_D at zero angle of attack in Fig. 5.2;
- The axial force coefficient C_A at 4° angle of attack in Fig. 5.3;
- The normal force coefficient C_N at 4° angle of attack in Fig. 5.4;
- Lift coefficient C_L at 8° angle of attack in Fig. 5.5.

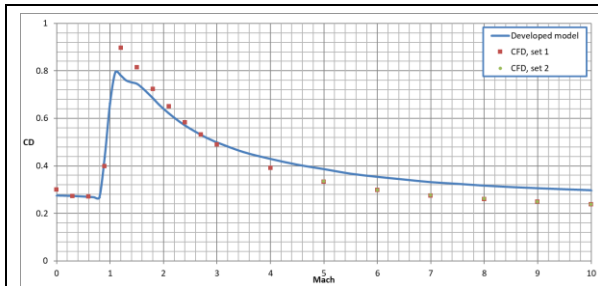


Fig. 5.2 Data comparison, drag coefficient, 0° angle of attack

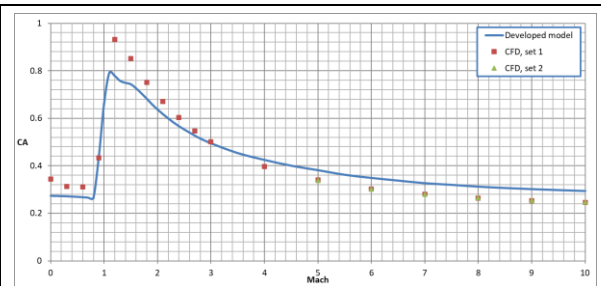


Fig. 5.3 Data comparison, axial force coefficient, 4° angle of attack

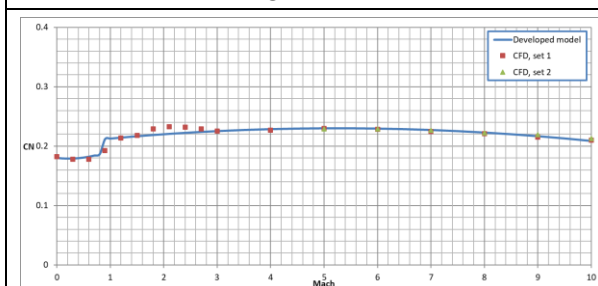


Fig. 5.4 Data comparison, normal force coefficient, 4° angle of attack

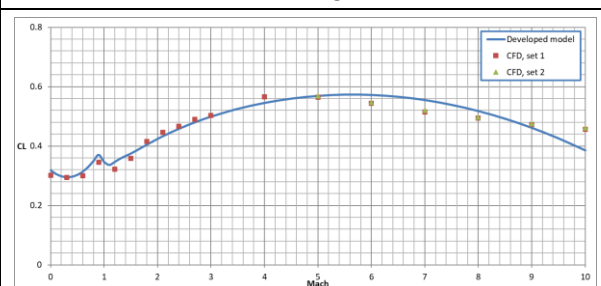


Fig. 5.5 Data comparison, lift coefficient, 8° angle of attack

The results obtained with the mathematical models presented in this chapter were compared with those obtained after the CFD investigations, observing a very good data correlation, despite of the reduced calculation time (0.1s/case - developed model vs. 24h/case - CFD model).

6 Study on the launcher dynamics and trajectory optimization

6.1 Overview

Obtaining the orbital performance of the launcher starting from a limited number of input data and optimization variables is done in the last main module of the MDO algorithm (according to Fig. 2.1). During the optimization process, the duration of key evolution phases changes iteratively, together with some parameters closely related to the control schemes.

6.2 Reference frames

Following the contents of [31], [32] the reference frames specific to the launcher motion have been defined, being grouped in:

- Frames independent of the Earth's rotation, which include: The Earth Frame ($OX_P Y_P Z_P$), The Inertial Local Frame ($OX_L Y_L Z_L$), The Inertial Start Frame ($OX_0 Y_0 Z_0$);
- Frames in which the trihedral is subjected to a rotational motion with the Earth or the launcher, which include: The Geocentric Spherical Frame ($O_P \lambda \varphi r$), The Geographical Mobile Frame ($Ox_g y_g z_g$), The Body Frame (Ox, y, z), The Velocity Frame or The Aerodynamic Frame ($Ox_a y_a z_a$) and The Quasi-Velocity Frame or The Trajectory Frame ($Ox_a^* y_a^* z_a^*$).

6.3 Coordinate transformations

After defining the reference frames, this section presents the rotation matrices from one frame to another, matrices that can be used to write equations of motion in any desired system.

6.4 Gravitational model

An important term that influences the motion of the launcher is the gravitational acceleration. This subchapter presents the J2 model, in which the components of gravitational acceleration (radial and polar) are calculated based on the current radius r and the geocentric latitude φ .

6.5 Dynamic models

Because the code developed for the *Trajectory* module (of motion dynamics and trajectory optimization) must include a fast mathematical model, a three degrees of freedom (3DOF) dynamic model was selected following the results of [31], the equation being written in the quasi-velocity frame. For a further validation of a baseline trajectory, a complex 6DOF dynamic model is used, being developed a second numerical code (flight simulator). Due to the very long computational time, the use of a complex dynamic model is not feasible in a multidisciplinary optimization problem.

6.5.1 Six degrees of freedom model – 6DOF

To write the equations of motion specific to the launcher, which is a body of variable mass, the theorems of impulse and kinetic momentum are applied. The model is detailed in [31], the main ideas being extracted in the thesis. The 6DOF dynamic system, for the case of the guided space launcher, totals 21 differential equations:

- 3 dynamic equations of translation using the quasi-velocity frame;
- 3 kinematic equation of translation using spherical coordinates;

- 3 dynamic equations of rotation around the center of mass using the body frame;
- 3 auxiliary equations to determine the aerodynamic angles;
- 6 kinematic equations of rotation (3 in the start frame and 3 in the geographical mobile frame);
- 3 equations for the TVC system dynamics.

6.5.2 Three degrees of freedom model – 3DOF

In preliminary design activities, when the technical information of the launcher is not fully outlined, and also in trajectory optimization applications, which require a large number of successive evaluations, it is recommended the use of a simplified dynamic model, with three degrees of freedom (3DOF), which describes only the translational motion of the launcher. To develop this simplified model, only the dynamic and kinematic translation equations (that describe the velocity and position of the launcher) from the complex 6DOF model are preserved. In the literature there are different implementations of the 3DOF model [31], in the thesis being used the model with zero roll-velocity angle μ .

The differential equations needed to be integrated for the 3DOF model are the following:

$$\begin{aligned}
\dot{V} &= \frac{N_x}{m} - g_r \sin \gamma - g_\omega (\cos \varphi \cos \chi \cos \gamma + \sin \varphi \sin \gamma) \\
\dot{\gamma} &= \frac{N_y}{mV} - \frac{g_r}{V} \cos \gamma - \frac{g_\omega}{V} (-\cos \varphi \cos \chi \sin \gamma + \sin \varphi \cos \gamma) + \frac{V}{r} \cos \gamma - 2\Omega_p \cos \varphi \sin \chi \\
\dot{\chi} &= -\frac{N_z}{mV \cos \gamma} + \frac{g_\omega \cos \varphi \sin \chi}{V \cos \gamma} + \frac{V}{r} \tan \varphi \sin \chi \cos \gamma + 2\Omega_p (\cos \varphi \cos \chi \tan \gamma - \sin \varphi) \\
\dot{\varphi} &= \frac{V}{r} \cos \chi \cos \gamma \\
\dot{\lambda} &= -\frac{V \sin \chi \cos \gamma}{r \cos \varphi} \\
\dot{r} &= V \sin \gamma
\end{aligned} \tag{6.1}$$

where: V is the launcher velocity (relative to the atmosphere), γ is the flight path angle, χ is the track angle, φ is the geocentric latitude, λ is the geocentric longitude (relative), N_x, N_y, N_z are the components of the applied force, m is the instantaneous mass of the launcher, g_r, g_ω are the components of gravitational acceleration and Ω_p is the angular velocity of the Earth.

The thrust orientation with respect to the velocity vector is described by the aerodynamic angles α and β^* , which can be seen as control parameters of the system with which the flight path angle γ , respectively track angle χ can be controlled using feedback relations such as:

$$\alpha = -k_1(\gamma - \gamma_d); \beta^* = -k_1(\chi - \chi_d) \tag{6.2}$$

where the reference (control desired) values are γ_d and χ_d , and k_1 is a setting parameter.

The launcher can be controlled exclusively by feedback relations of type (6.2), both for the primary active guidance phase and for the orbital insertion phase. A better solution is to use a method based on optimal commands in the orbital injection phase, as developed in [31]:

$$\alpha = -k_2(\gamma - \delta_1); \beta^* = -k_3(i - i_d) \tag{6.3}$$

where i_d represents the target orbit inclination, k_2 and k_3 are setting parameters, and δ_1 is the command in the orbit-related reference system obtained by optimizing the orbital injection maneuver (decrease of orbit eccentricity to zero in minimum time for a circular orbit).

6.6 Orbital parameters

In order to perform a correct orbital performance analysis specific to the trajectory obtained after integrating the system of 6 differential equations corresponding to the 3DOF model used, it is necessary to convert the position vector \vec{r} and velocity vector \vec{v} into classical orbital parameters $a, e, i, \Omega, \omega, f$ (semimajor axis, eccentricity, inclination, longitude of ascending node, argument of periapsis and true anomaly). The first two parameters, together with the fifth, define the trajectory of the body in a plane, the next two define the orientation of the plane in space, and the last one defines the position of the body in orbit. Within this subchapter the 6 orbital parameters are detailed, being also presented the related mathematical models.

6.7 Launcher evolution phases

The way in which the trajectory is optimized is closely related to the altitude of the orbit and the mass of the payload, the evolution phases being different depending on the insertion method. For small launchers, predominantly, it is preferred the use of a direct trajectory (DATO - Direct Ascent To Orbit), because it does not involve successive stops and restarts of the upper stage engine. At the same time, the time required for the launcher mission is reduced.

The key events and evolution phases specific to a typical small launcher mission (with a two-stage architecture) using a DATO trajectory are: Vertical evolution, Primary active guidance (non-zero aerodynamic angles), Primary gravitational turn (zero aerodynamic angles), Separation of the first stage, Separation of the fairing, Ignition of the second stage engine, Secondary gravitational turn, Final active guidance (orbital insertion), ending with the separation of the satellite from the upper structure. These are shown in Fig. 6.1.

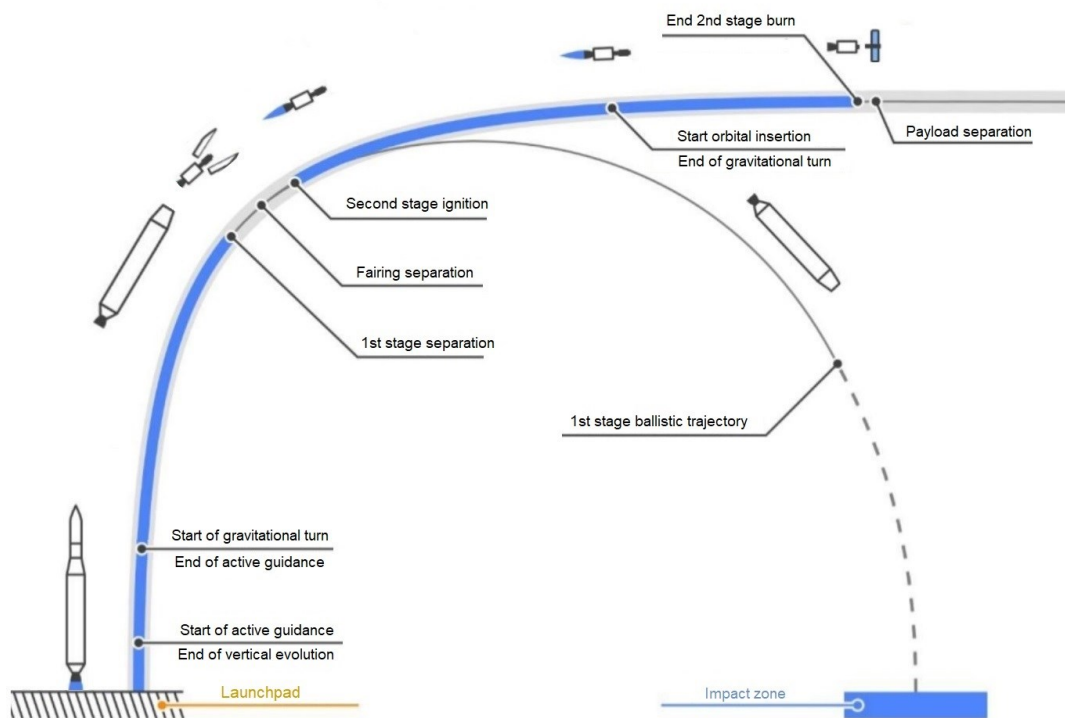


Fig. 6.1 Key events and evolution phases, two-stage launcher - DATO trajectory

6.8 Auxiliary data

In order to fully analyze the launcher's performance, it is necessary to define an additional set of data. These data are known as auxiliary data, the most important being the load factors (axial and normal) and the heat flux at the stagnation point.

6.9 Validation of the model

For the validation of the simulator developed for the *Trajectory* module, and also for the trajectory optimization code (the *Weights and Sizing* and *Propulsion* modules are deactivated from the MDO algorithm) the small launcher configurations Falcon 1 and Falcon 1e were used. Reference data and orbital performance corresponding to 9.1° inclination circular orbits, DATO trajectories were obtained from [33]. The aim was to minimize the objective function detailed in relation (7.7), which is equivalent to maximizing the payload mass that can be inserted in a predefined orbit. An adaptive Runge-Kutta 5(4) method was used to integrate the equations of motion.

A representative example of the quality of the obtained orbits (Falcon 1e) is presented in Fig. 6.2. The variation of the altitude with time can be observed, with a continuous line being presented the trajectory of the launcher, and with a dashed line the trajectory of the satellite. Maintaining a constant altitude after the satellite detachment from the upper structure confirms the circularity of the orbit achieved.

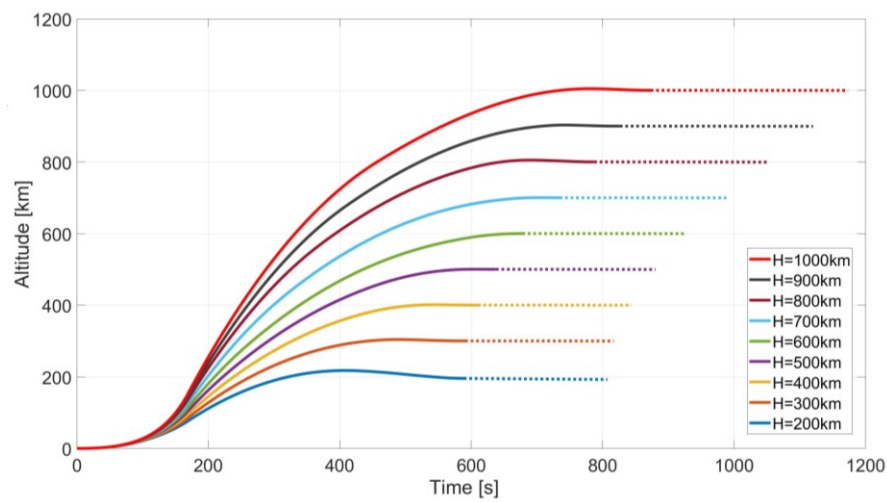


Fig. 6.2 Falcon 1e, different missions, altitude vs. time

Comparing the reference orbital performance of the launchers with those obtained with the developed method, an average error of 5.46% was observed for Falcon 1 (5 missions) and an average error of 7.71% for Falcon 1e (9 missions), thus the overall average error is 6.91%. A higher payload was obtained after optimizing the reference trajectories for 12 of the 14 studied cases. The numerical results are presented in Fig. 6.3.

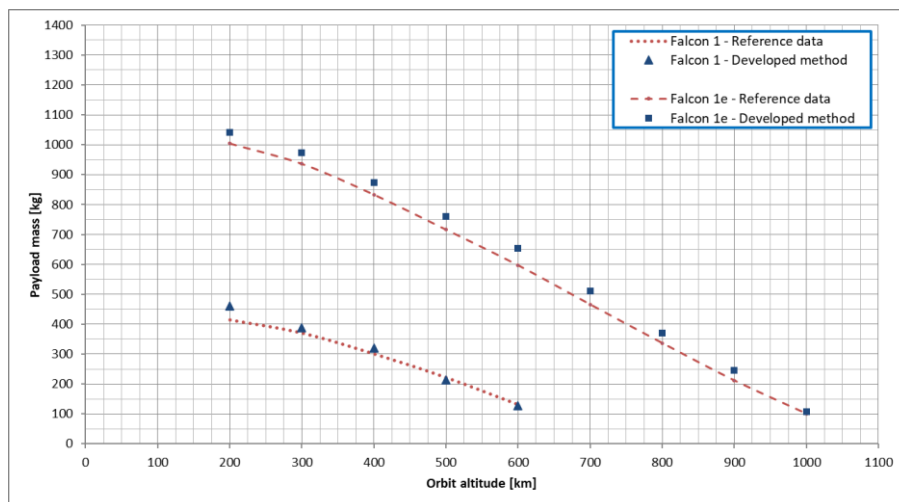


Fig. 6.3 Data comparison, Falcon 1 and Falcon 1e performance, $e = 0$, $i = 9.1^\circ$

7 Additional details on the multidisciplinary optimization algorithm

7.1 Solution selection and advancement algorithm

In order to decide on the solution selection and advancement algorithm within the iterative MDO process, an analysis was performed on 21 classical optimization problems (with multiple local minimums, e.g. Rastrigin function), being studied a gradient algorithm (interior point), one heuristic algorithm (genetic) and a hybrid algorithm (combination of previous two). According to the analysis detailed in the thesis, the most suitable algorithm proved to be the hybrid one, which managed to first take advantage of the genetic algorithm by obtaining a significant narrowed search field, and then the advantage of the gradient algorithm, that of converging to a solution characterized by a smaller objective function (having now a very good initial solution).

7.2 Optimization variables

The process of launcher global optimization is equivalent to the optimization of several key parameters (optimization variables), the launcher being then completely defined through them and the global input data. The optimization variables are directly necessary for the mathematical models used in the disciplinary analyses developed in chapters 3-6. It was considered, where the implementation was convenient, a dimensionless formulation of these key parameters in order to reduce as much as possible the search space/field of the optimal solution.

Thus, for the case of a 2-stage liquid propellant small launcher, the following optimization variables are used:

a) For the first stage definition (5 variables in total):

- Propellant mass (oxidizer + fuel) of the first stage, M_{p_1} ;
- The outer diameter of the first stage, D_{e_1} ;
- The combustion chamber pressure of the first stage engine, P_{c_1} ;
- The exhaust pressure of the first stage engine, P_{e_1} ;
- Thrust to Weight ratio at the start of the first stage burn, $\left(\frac{T}{W}\right)_1$.

b) For the second stage definition (5 variables in total):

- Propellant mass (oxidizer + fuel) of the second stage, M_{p_2} ;
- The outer diameter of the second stage, D_{e_2} ;
- The combustion chamber pressure of the second stage engine, P_{c_2} ;
- The exhaust pressure of the second stage engine, P_{e_2} ;
- Thrust to Weight ratio at the start of the second stage burn, $\left(\frac{T}{W}\right)_2$.

c) For the trajectory definition (6 variables in total):

- Duration of vertical ascent after launch sequence, $t_{vertical}$;
- Duration of coasting between first stage separation and second stage ignition, t_{coast} ;
- The desired flight path angle for the first stage control, γ_{d_1} ;
- The desired track angle for the first stage control, χ_{d_1} ;
- Ratio between active guidance time and total guidance time (active + gravitational) for the first stage, Δt_1 ;
- Ratio between active guidance time and total guidance time (active + gravitational) for the second stage, Δt_2 .

A total of 16 optimization variables is required for a preliminary design of an optimal constructive solution for a 2-stage launcher. According to the optimization vector structure detailed in the thesis, for a launcher with n stages ($n \geq 2$), in total $9n - 2$ optimization variables are required. If only the maximization of the inserted payload into a desired orbit with the aid of an imposed launcher is considered (only the optimization of the trajectory, see chapter 6), then the complexity of the problem decreases significantly (only $4n - 1$ optimization variables are needed), being no need for the use of the *Weights and Sizing* and *Propulsion* modules. The launcher geometry, required for the *Aerodynamics* module, is fully defined prior to the trajectory optimization, but in addition, there is a need to introduce the payload mass $m_{payload}$ as an optimization variable.

7.3 Requirements and input data

The different inputs required for the MDO algorithm are defined prior to its execution, the most important being the requirements of the target orbit, the constraints to be applied, the problem analysis area limits (solution search space), the launch location, the fairing separation condition and the materials used, together with their mechanical and thermal properties.

7.4 Objective function

The objective function defines the criteria according to which the solution is advanced (the optimization variables vector). Examples of possible objective function formulations appropriate to small space launchers are minimizing the lift-off mass, minimizing the vehicle cost, maximizing the payload performance index (payload to lift-off mass ratio), or maximizing the payload mass (if the vehicle is already defined). The current trend is miniaturization, so an objective function is implemented in which the dominant criteria is the minimum mass at the start of the mission (also known as GLOW – Gross lift-off weight).

The objective function used in the thesis is the following:

$$f_{objective} = (M_{start} + I_{orbit}) \cdot I_{constraints} \quad (7.1)$$

where M_{start} is the launcher lift-off mass, I_{orbit} is the target orbit index, and $I_{constraints}$ is the imposed constraints index.

The target orbit index quantifies the quality of the orbit obtained compared to that imposed before launch. Thus, it is of interest to introduce in the formula definition the orbital parameters presented in subchapter 6.6. The formulation used to compute I_{orbit} , for a circular orbit of target inclination i_{target} and target altitude H_{target} is:

$$I_{orbit} = \sqrt{w_a(a - a_{target})^2 + w_v(V_i - V_{target})^2 + w_\gamma(\gamma - \gamma_{target})^2 + w_i(i - i_{target})^2} \quad (7.2)$$

The target semimajor axis a_{target} is computed using:

$$a_{target} = R_p + H_{target} \quad (7.3)$$

where R_p is the Earth reference radius.

The target velocity (inertial) V_{target} , for a circular orbit is computed using:

$$V_{target} = \sqrt{\frac{\mu}{r_{target}}} = \sqrt{\frac{\mu}{a_{target}}} \quad (7.4)$$

where μ is the standard gravitational parameter.

Finally, the target flight path angle is $\gamma_{target} = 0$ for a circular orbit. The target orbit eccentricity $e_{target} = 0$ was replaced with V_{target} and $\gamma_{target} = 0$ for a faster solution convergence. The parameters a, V_i, γ, i are obtained following the numerical integration of the dynamic model, the data corresponding to payload detachment being used (the relative velocity V from the quasi-velocity non-inertial frame is converted to V_i in Earth initial frame - ECI).

For the parameter weights associated with (7.2) the following values have been used:

$$w_a = w_V = 1; w_\gamma = w_i = 10 \quad (7.5)$$

For a correct insertion into target orbit, the index I_{orbit} tends to null value (the value 0 is assigned to an ideal insertion).

The imposed constraints index is used to quantify the validity of the obtained trajectory in relation to the imposed constraints and requirements. The formula used for $I_{constraints}$, with a number of $N_{constraints}$ is the following:

$$I_{constraints} = \prod_{i=1}^{N_{constraints}} I_{constraints_i} \quad (7.6)$$

where $I_{constraints_i}$ is the constraint index corresponding to the i^{th} constraint.

The imposed constraints depend strictly on the nature of the studied problem, for the optimization of the launcher configuration and implicitly the trajectory according to the evolution phases mentioned previously, one can use:

- Constraints for the load factors to which the launcher is subjected during the mission;
- Constraints for excluding negative transitions from the launcher architecture;
- Constraints for respecting the allowed variation of diameter between consecutive stages;
- Constraints for maximum stage fineness ratio;
- Constraints for nozzle expansion ratio;
- Constraints for achieving the desired control parameters γ_a and χ_a during the active guidance phase;
- Constraints for the alignment of the thrust vector with the velocity vector at the end of active guidance phase.

If the constraints are not respected, the terms $I_{constraints_i}$ associated with these constraints would take over-unit values, which would increase the objective function numerical value. If the constraint is met, then the term $I_{constraints_i}$ would take the value 1. In addition, a main constraint is implemented, having a value much higher than the others mentioned above, being used $I_{constraints_i} = 10^5$. This is only used if the trajectory is not computed until the end of the mission (for example the trajectory was sub-orbital, the launcher returning to Earth, $H < 0$) to remove the respective optimization vectors from the future population.

If only the maximization of the inserted payload mass with the aid of an imposed launcher is considered (only the optimization of the trajectory, see chapter 6), then the objective function implemented is the following:

$$f_{objective} = \left(\frac{m_{reference}}{m_{payload}} + I_{orbit} \right) \cdot I_{constraints} \quad (7.7)$$

where $m_{reference}$ is the reference payload mass (obtained from the launcher manual), and $m_{payload}$ is the maximum achieved payload mass (optimization variable).

8 Optimization of a nominal launcher constructive solution

8.1 Preliminary design requirements

Initially, the multidisciplinary optimization algorithm developed in the thesis was used to obtain a launcher optimal constructive solution (from a mass point of view) for a baseline mission. The mission defined by the requirements in Table 8.1 was used, the most important input data being presented in Table 8.2.

Table 8.1 Target mission requirements

Requirement	Specification
Orbit type	Circular
Target altitude	400 km
Target inclination	Polar (90°)
Payload mass	130 kg

Table 8.2 Small launcher input data

Input	Specification
Number of stages	2
Launcher architecture	Constant diameter
Oxidizer	Liquid Oxygen (O_2)
Fuel	Liquid Methane (CH_4)

The launch location used was the Andøya Space Center platform (Norway), which is the preferred one for obtaining polar orbits due to its high launch latitude. Additional input data, constraints and control schemes are presented in detail in the thesis. The search limits for the 16 optimization variables were very broad, a large initial space being desired not to exclude the optimal solution. For example: for the first stage propellant mass, the analyzed search interval was $M_{p_1} \in [5t, 25t]$; for the lift-off thrust to weight ratio, the search interval was $\left(\frac{T}{G}\right)_1 \in [1, 5]$; for the duration of vertical ascent, the search interval was $t_{vertical} \in [2s, 100s]$.

8.2 Convergence of the developed algorithm

For the nominal case convergence, a number of 1625 generations were performed with the genetic algorithm. The solution was not further improved with the gradient-based algorithm. An initial population of 100 individuals was used, so the total number of iterations required to optimize the nominal launcher was 162500 iterations. The duration of an iteration was about 0.5 s, so the time required for launcher optimization totaled about 22 hours.

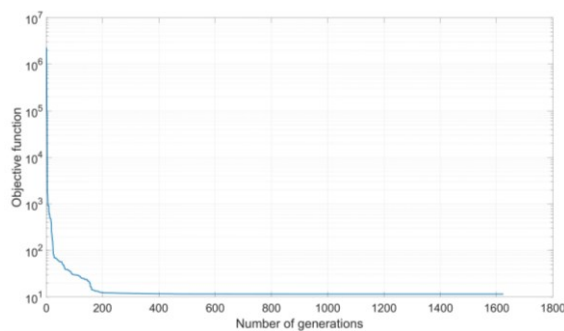


Fig. 8.1 Objective function convergence, nominal case

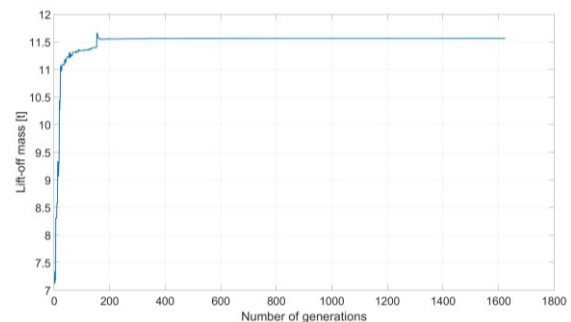


Fig. 8.2 Lift-off mass convergence, nominal case

The convergence of the objective function is presented in Fig. 8.1. Only the best solution of the current generation is displayed, a decrease in time to the minimum value being observed. At the end of the multidisciplinary optimization process, the minimum value found was $f_{objective} = 11.5687$. A sudden decrease in the value of the objective function in the first hundreds of generations can be observed. After that, a slow process of solution refinement towards the optimal value begins.

In Fig. 8.2 the convergence of the launcher lift-off mass (together with the payload) can be observed. Due to the way in which the work strategy was implemented (objective function, target orbit index, imposed constraints index), there is an increase in the mass of the launcher to the minimum value. This is beneficial to the final result, because there is a lower risk that the solution obtained is a local minimum and not the global one. At the end of the multidisciplinary optimization process, the minimum value $M_{start} = 11.5642$ [t] was found. At solution convergence, a target orbit index of $I_{orbit} = 0.0045$ was obtained, corresponding to a very good insertion. All imposed constraints were met, so $I_{constraints} = 1$. The numerical values obtained for the optimization variables from the MDO algorithm are presented in detail in the thesis.

8.3 Constructive solution

With the aid of the optimization variables obtained following the convergence of the iterative MDO process, the entire constructive solution of the small launcher can be generated, according to the model implemented in the *Weights and Sizing* module. The general details regarding the specifications of the constructive solution generated can be observed in Table 8.3, the main constructive components of the launcher being presented in Fig. 8.3.

Table 8.3 Nominal launcher, general specifications

Specification	Value
Lift-off mass [t]	11.56
Payload performance index [%]	1.12
Total length [m]	17.64
Outer diameter [m]	1.35
Payload mass [kg]	130
Upper structure mass [kg]	219.71
Upper structure length [m]	2.02
Propellant	$O_2 + CH_4$
First stage mass [t]	9.93
First stage length [m]	12.17
First stage burn time [s]	112.68
First stage mean thrust [kN]	236.82
Second stage mass [t]	1.41
Second stage length [m]	3.45
Second stage burn time [s]	386.57
Second stage mean thrust [kN]	10.97

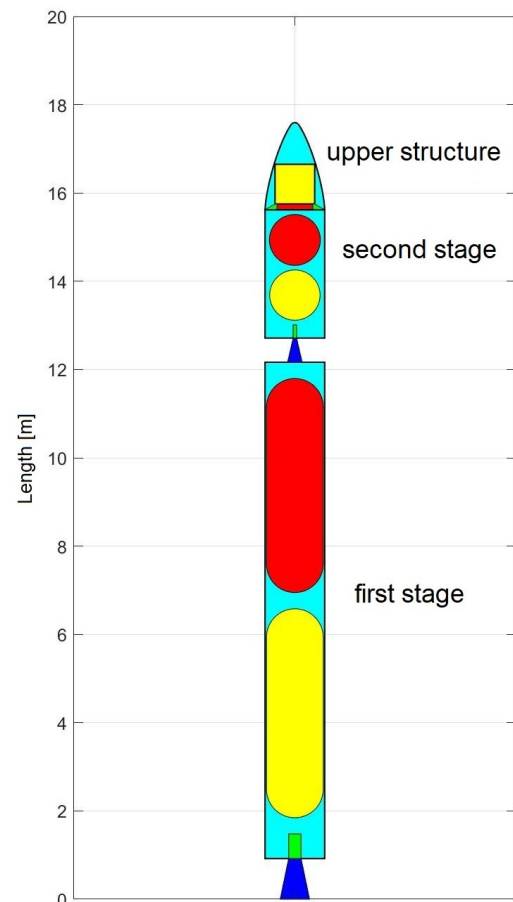


Fig. 8.3 Nominal launcher main components

The color code for the interior components of the launcher is the following:

- For stages: oxidizer tank (red), fuel tank (yellow), combustion chamber (green), nozzle (blue);
- For upper structure: fairing (cyan), payload (yellow), adapter (green), VEB (red).

8.4 Baseline trajectory

The multidisciplinary optimization algorithm developed in the thesis, in addition to optimizing a small launcher constructive solution, simultaneously defines the reference trajectory that needs to be followed in order to fulfill the mission. The durations of the evolution phases related to the baseline mission are presented in Table 8.4, a total of approximately 8.5 minutes being needed to accomplish it. The deviation from the imposed target parameters is presented in Table 8.5. An increased accuracy can be observed in reaching the target orbit, this aspect being also visible from the value of the target orbit index ($I_{orbit} = 0.0045$).

Table 8.4 Baseline mission phases

Evolution phase	Duration [s]
Vertical flight	10.81
Primary active guidance	33.22
Primary gravitational turn	68.64
Coast after stage separation	12.92
Secondary gravitational turn	259.28
Orbit insertion	127.29
TOTAL mission	512.18

Table 8.5 Insertion errors, nominal launcher

Target parameter	Insertion error
Semimajor axis a_{target} [km]	$-4.18 \cdot 10^{-6}$
Eccentricity e_{target} [-]	$5.43 \cdot 10^{-7}$
Orbit inclination i_{target} [°]	$4.45 \cdot 10^{-4}$
Inertial velocity V_{target} [m/s]	$-2.46 \cdot 10^{-5}$
Flight path angle γ_{target} [°]	$3.11 \cdot 10^{-5}$

Fig. 8.4 - Fig. 8.6 shows the variation in time of certain parameters used in the objective function formulation. Because the desired orbit is circular, the eccentricity obtained is zero. For the trajectory flight path angle one can observe the primary active guidance phase, culminating in a period in which the angle γ is quasi-constant. For the orbit inclination, a small correction can be observed during the orbital insertion maneuver to obtain a 90° inclination at the time of satellite detachment. The mass evolution over time is shown in Fig. 8.7.

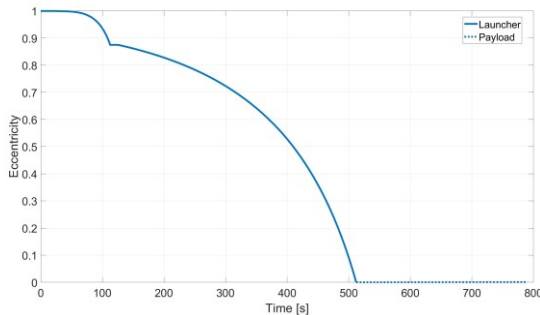


Fig. 8.4 Nominal launcher, baseline trajectory, eccentricity vs. time

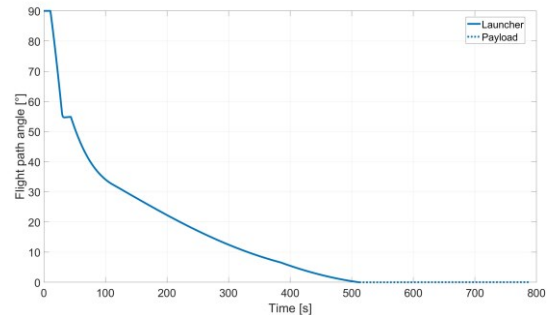


Fig. 8.5 Nominal launcher, baseline trajectory, flight path angle vs. time

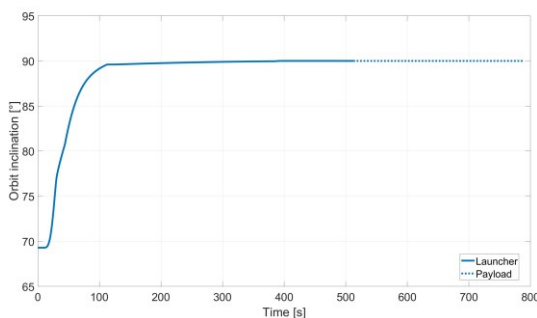


Fig. 8.6 Nominal launcher, baseline trajectory, orbit inclination vs. time

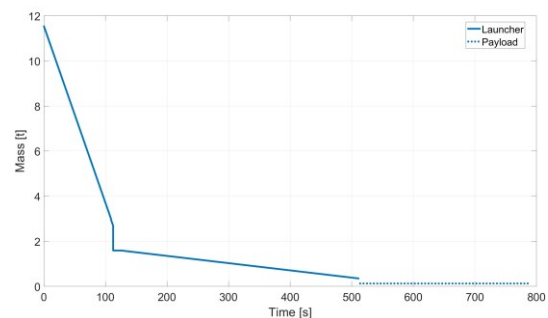


Fig. 8.7 Nominal launcher, baseline trajectory, mass vs. time

8.5 Mission validation

Within the MDO algorithm, the dynamic model used is a simplified 3DOF type (with null roll-velocity angle), totaling 6 differential equations. To validate the baseline trajectory, a complex 6DOF dynamic model was used, consisting of 21 differential equations. Using the 6DOF motion simulator developed, a much more realistic trajectory was obtained, being analyzed also the motion around the launcher center of mass.

The pitch angular velocity is shown in Fig. 8.8, while the required pitch command (TVC deflection) can be seen in Fig. 8.9. The two active guidance zones are observed, the maximum angular velocity being approximately $16^\circ/\text{s}$ at the start of launcher pitch-over maneuver.

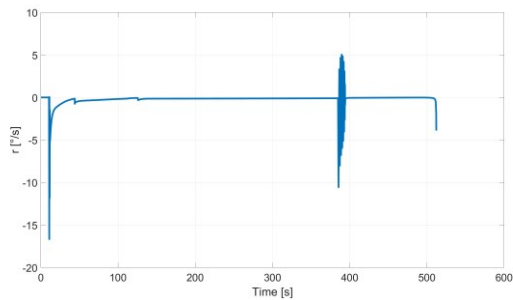


Fig. 8.8 Pitch angular velocity (r) around the center of mass

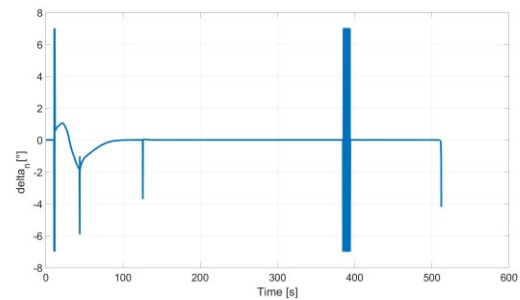


Fig. 8.9 Pitch command (TVC deflection)

For the lateral control of the launcher, the number and magnitude of the associated commands are much smaller, the launcher requiring only minor corrections to achieve the target inclination. The yaw angular velocity is shown in Fig. 8.10, while the required yaw command (TVC deflection) can be observed in Fig. 8.11.

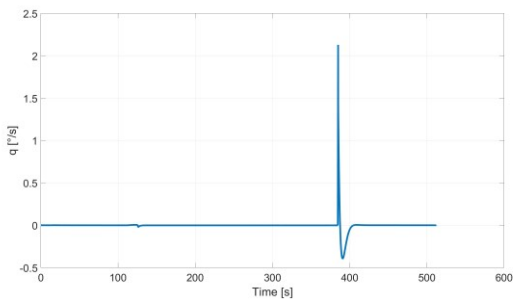


Fig. 8.10 Yaw angular velocity (q) around the center of mass

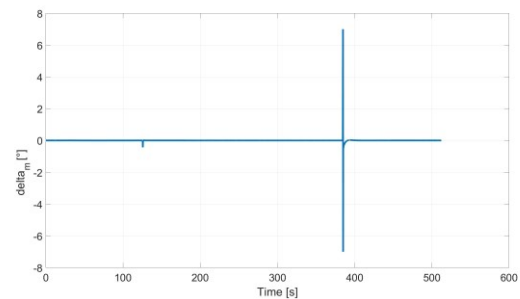


Fig. 8.11 Yaw command (TVC deflection)

Following the use of the 6DOF motion simulator it was confirmed that the trajectory generated using the simplified 3DOF model is a feasible one, two comparisons of interest (variation of altitude and inclination in time) being presented in Fig. 8.12 and Fig. 8.13.

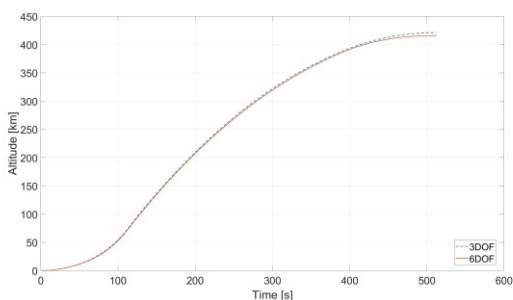


Fig. 8.12 Trajectory validation, altitude vs. time

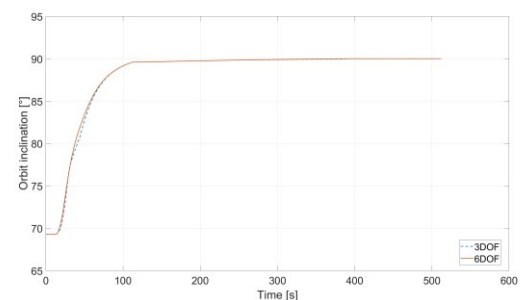


Fig. 8.13 Trajectory validation, orbit inclination vs. time

9 Parametric analysis regarding small launchers

9.1 Target orbit altitude impact

In this subchapter the impact of the target orbit altitude on the small launcher was studied, being analyzed 5 missions, with altitudes of the circular, polar, target orbit between 200 and 600 km, with increments of 100 km. The payload mass was 130 kg. Some of the general details regarding the specifications of the obtained constructive solutions are observed in Table 9.1, while the main components are presented graphically in Fig. 9.1.

Table 9.1 General details small launchers, orbit altitudes 200-600 km

Specification	Value				
	H=200km	H=300km	H=400km	H=500km	H=600km
Lift-off mass [t]	9.92	10.80	11.56	12.89	13.96
Payload performance index [%]	1.31	1.20	1.12	1.01	0.93
Total length [m]	16.78	17.54	17.64	18.31	19.07
Outer diameter [m]	1.27	1.29	1.35	1.4	1.41
Payload mass [kg]	130	130	130	130	130
Propellant	$O_2 + CH_4$	$O_2 + CH_4$	$O_2 + CH_4$	$O_2 + CH_4$	$O_2 + CH_4$
First stage burn time [s]	117.64	129.17	112.68	102.09	96.96
First stage mean thrust [kN]	189.51	198.86	236.82	293.74	332.89
Second stage burn time [s]	328.69	401.62	386.57	439.57	490.8
Second stage mean thrust [kN]	12.2	7.75	10.97	10.14	11.2

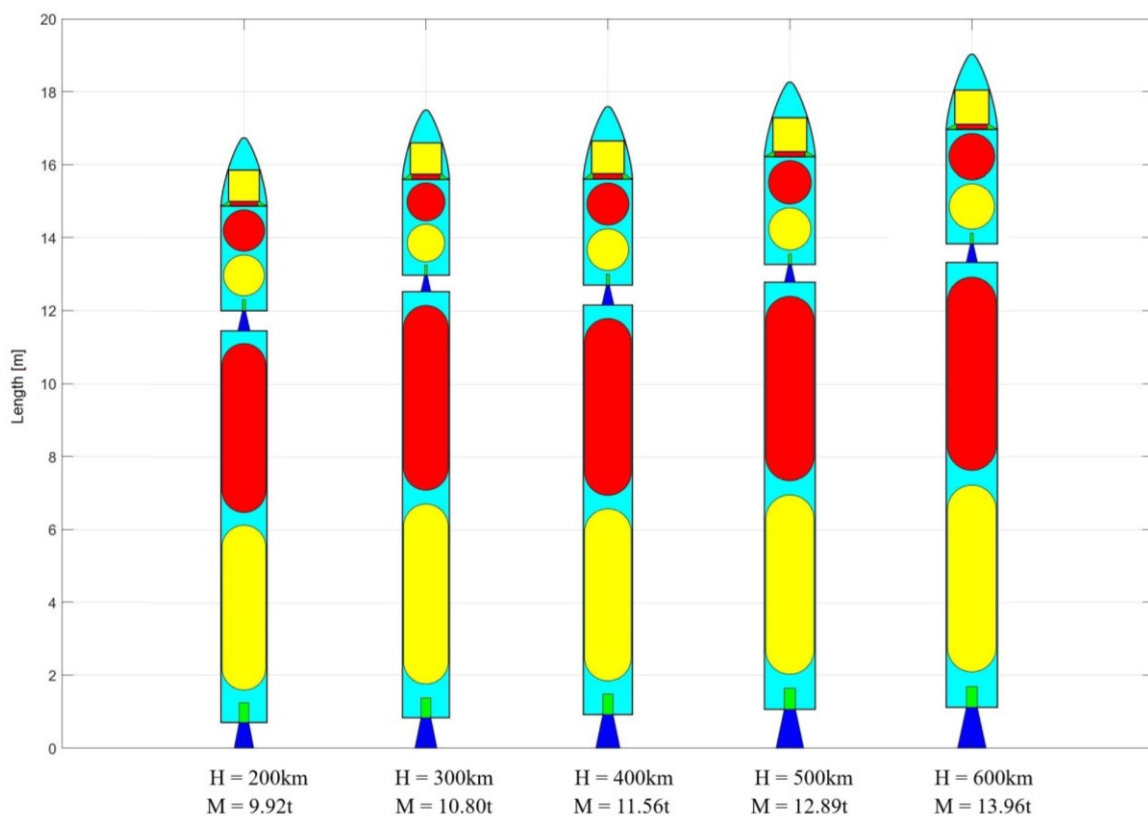


Fig. 9.1 Launcher main components, orbit altitudes 200-600 km

9.2 Payload mass impact

In this section the impact of the payload mass on the small launcher was studied, being analyzed 9 missions, with payload masses (m) between 10 and 250 kg, with increments of 30 kg. The altitude of the circular, polar, target orbit was 400 km. Some of the general details regarding the specifications of the obtained constructive solutions are observed in Table 9.2, while the main components are presented graphically in Fig. 9.2.

Table 9.2 General details small launchers, payload masses 10-250 kg

Specification	Value								
	m=10kg	m=40kg	m=70kg	m=100kg	m=130kg	m=160kg	m=190kg	m=220kg	m=250kg
Lift-off mass [t]	4.97	7.30	8.43	10.18	11.56	13.79	15.79	17.38	18.93
Payload performance index [%]	0.20	0.55	0.83	0.98	1.12	1.16	1.20	1.27	1.32
Total length [m]	10.59	12.90	14.35	16.54	17.64	19.16	20.34	21.19	21.72
Outer diameter [m]	1.35	1.37	1.37	1.33	1.35	1.39	1.43	1.47	1.51
Payload mass [kg]	10	40	70	100	130	160	190	220	250
Propellant	$O_2 + CH_4$	$O_2 + CH_4$	$O_2 + CH_4$	$O_2 + CH_4$	$O_2 + CH_4$	$O_2 + CH_4$	$O_2 + CH_4$	$O_2 + CH_4$	$O_2 + CH_4$
First stage burn time [s]	102.64	102.72	97.5	94.50	112.68	108.15	119.64	102.90	103.14
First stage mean thrust [kN]	109.71	161.16	196.71	239.46	236.82	290.65	303.46	376.04	414.45
Second stage burn time [s]	382.67	379.83	392.69	379.25	386.57	471.71	404.76	388.36	382.61
Second stage mean thrust [kN]	4.28	7.02	8.07	11.90	10.97	11.40	14.53	20.15	20.84

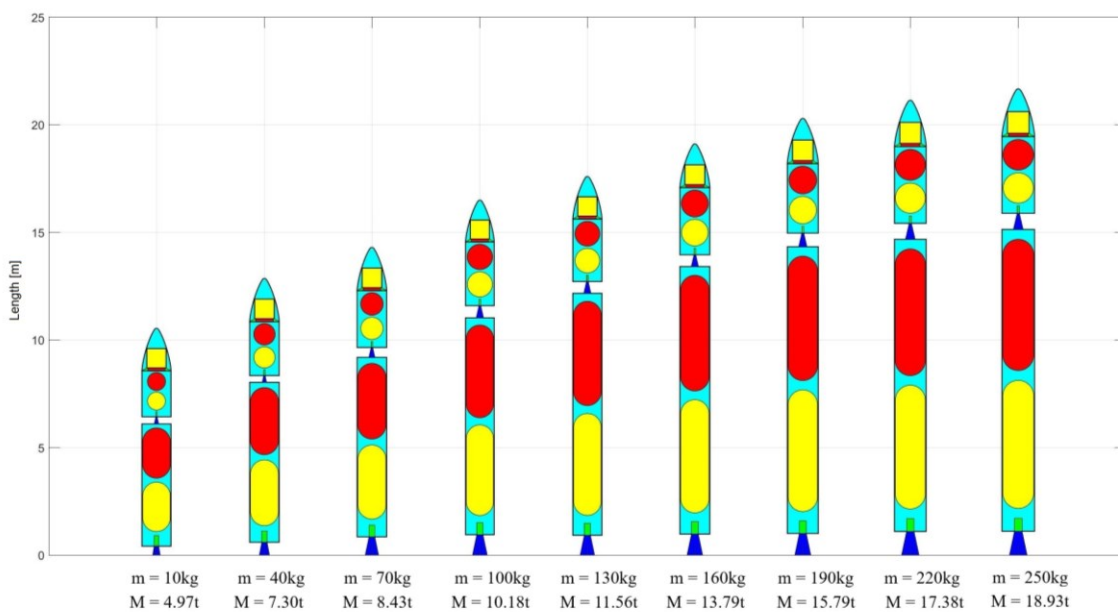


Fig. 9.2 Launcher main components, payload masses 10-250 kg

9.3 Typical missions impact

In this subchapter the impact of the typical missions on the small launcher was studied, analyzing 5 missions, with different launch locations and target orbit inclinations, specific to the approximately equatorial orbits, the International Space Station (ISS) orbit, the polar orbit, but also Sun-synchronous orbit (SSO). An altitude of 400 km was considered for all studied missions. The payload was considered 130 kg. Some of the general details regarding the specifications of the obtained constructive solutions are observed in Table 9.3, while the main components are presented graphically in Fig. 9.3.

Table 9.3 General details small launchers, typical missions

Specification	Value				
	Kourou $i = 5.3^\circ$	Omelek $i = 9.1^\circ$	Baikonur $i = 51.6^\circ$	Andøya $i = 90^\circ$	Andøya $i = 97.03^\circ$
Lift-off mass [t]	8.36	8.52	9.73	11.56	12.06
Payload performance index [%]	1.56	1.53	1.34	1.12	1.08
Total length [m]	16.06	16.17	16.33	17.64	18.13
Outer diameter [m]	1.18	1.19	1.29	1.35	1.35
Payload mass [kg]	130	130	130	130	130
Propellant	$O_2 + CH_4$	$O_2 + CH_4$	$O_2 + CH_4$	$O_2 + CH_4$	$O_2 + CH_4$
First stage burn time [s]	104.67	103.68	115.31	112.68	118.34
First stage mean thrust [kN]	185.5	192.35	199.86	236.82	242.69
Second stage burn time [s]	405.18	401.96	401.18	386.57	392.47
Second stage mean thrust [kN]	6.54	6.32	6.89	10.97	8.80

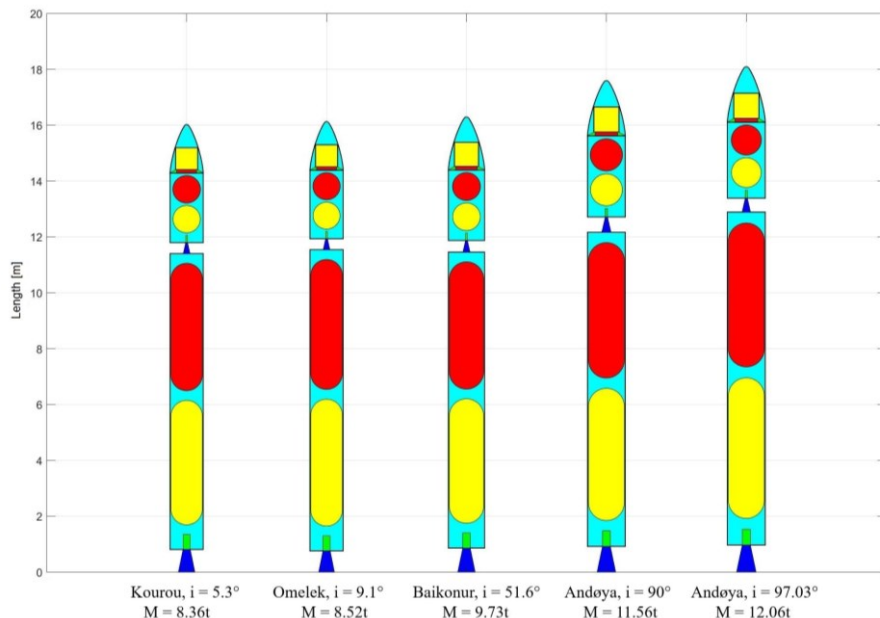
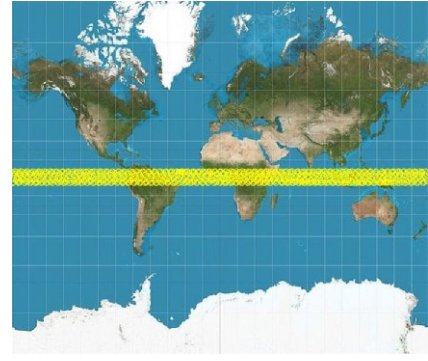
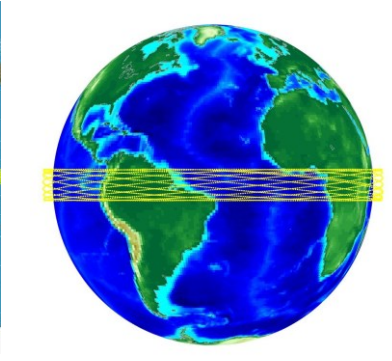
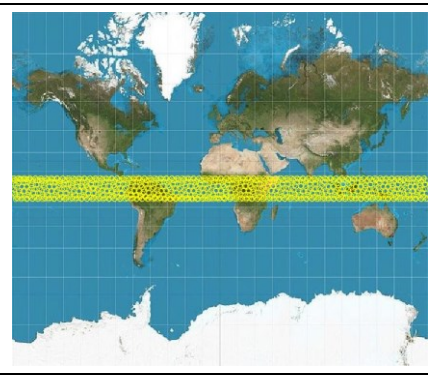
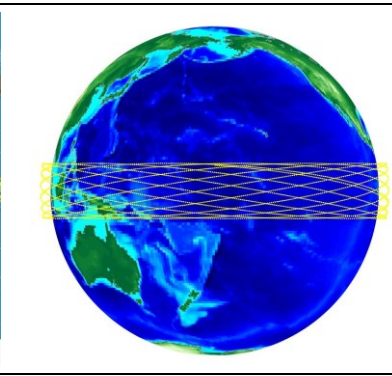
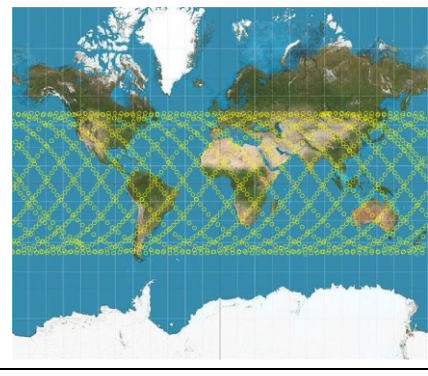
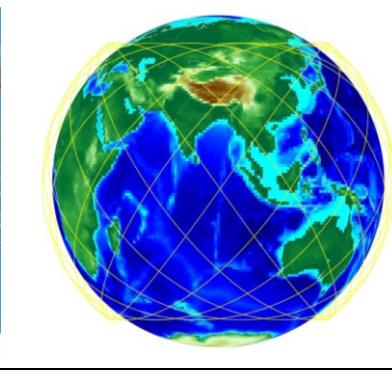
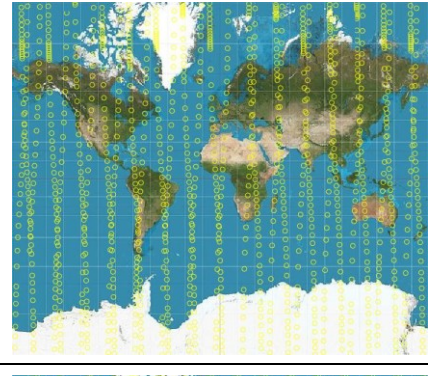
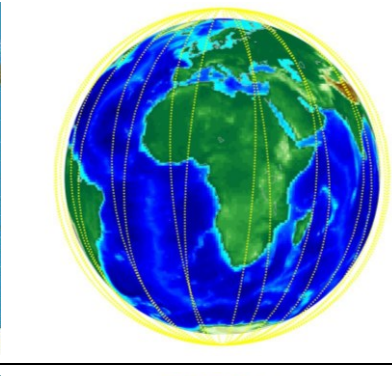
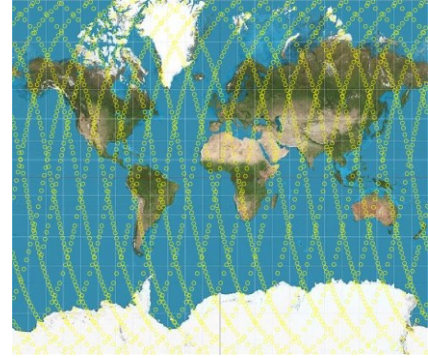
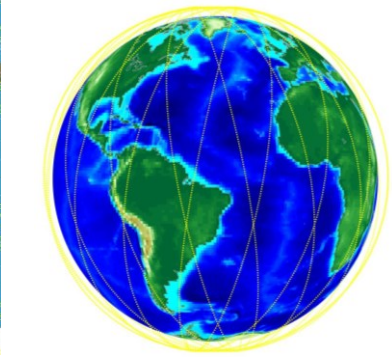


Fig. 9.3 Launcher main components, typical missions

The different inclinations of the target orbit allow the satellite inserted in it to view more or less extensive areas of the Earth. This aspect is strongly visible if one uses a graphical representation of the satellite orbital trajectory on a Mercator projection (2D) and one on the globe (3D), according to those presented in Table 9.4.

Table 9.4 Satellite trajectories 24h after insertion, typical missions (2D and 3D representations)

		<p>Mission 1, Kourou launch, Inclination = 5.3°</p>
		<p>Mission 2, Omelek launch, Inclination = 9.1°</p>
		<p>Mission 3, Baikonur launch, Inclination = 51.6°</p>
		<p>Mission 4, Andøya launch, Inclination = 90°</p>
		<p>Mission 5, Andøya launch, Inclination = 97.03°</p>

9.4 Used propellant impact

In this section the impact of the propellant used on the small launcher was studied, being analyzed a total of 4 pairs of liquid propellants, having as an oxidizer liquid oxygen and liquid fuel hydrogen (Launcher H-H), methane (Launcher M-M), kerosene (Launcher K-K) and ethanol (Launcher E-E). The target orbit was considered the baseline, circular, polar one of 400 km altitude, the payload being 130 kg. Some of the general details regarding the specifications of the obtained constructive solutions are observed in Table 9.5, while the main components are presented graphically in Fig. 9.4.

Table 9.5 General details small launchers, different propellant

Specification	Value			
	Launcher H-H	Launcher M-M	Launcher K-K	Launcher E-E
Lift-off mass [t]	6.51	11.56	15.07	26.96
Payload performance index [%]	2.00	1.12	0.86	0.48
Total length [m]	15.99	17.64	18.61	23.26
Outer diameter [m]	1.58	1.35	1.30	1.64
Payload mass [kg]	130	130	130	130
Propellant	<i>O₂ + hydrogen</i>	<i>O₂ + methane</i>	<i>O₂ + kerosene</i>	<i>O₂ + ethanol</i>
First stage burn time [s]	123.18	112.68	111.55	104.04
First stage mean thrust [kN]	138.31	236.82	293.20	552.19
Second stage burn time [s]	379.26	386.57	372.33	377.22
Second stage mean thrust [kN]	9.74	10.97	15.72	19.05

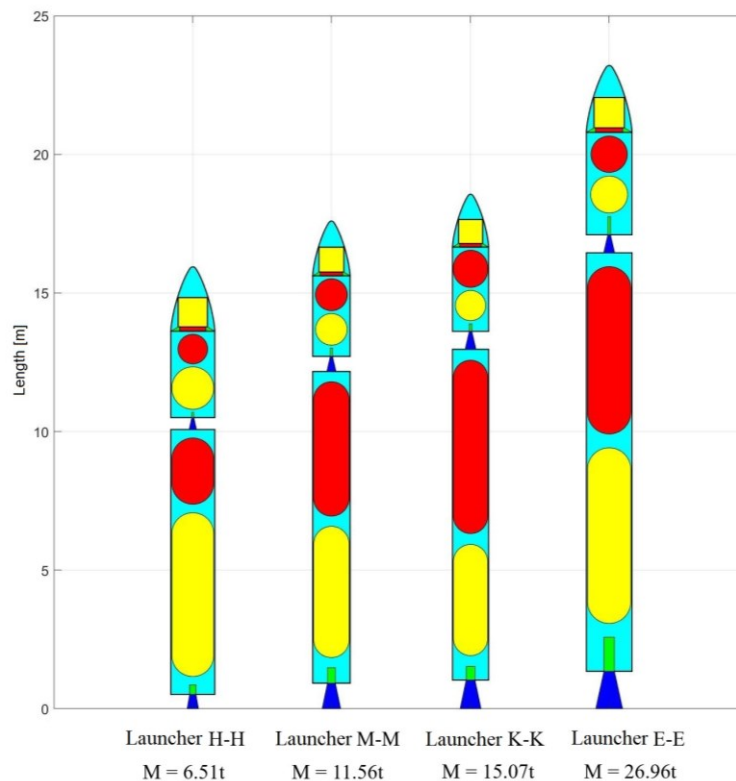


Fig. 9.4 Launcher main components, different propellant

10 Conclusions

10.1 Thesis contributions

The following contributions were brought in the thesis:

1. Development of a computational algorithm for the sizing and weights assessment of small launcher configurations, based on a bottom-up strategy, using a limited number of input data. For the fairing mass estimation, relation (3.1) is developed.
2. Development of a computational algorithm for estimating the propulsive performance of liquid propellant rocket engines. Nonlinear approximation functions of the form (4.2) were developed to compute the optimal mixture ratio between oxidizer and fuel, flame temperature, relative molecular weight and the gas specific heat ratio.
3. Development of a computational algorithm for the determination of aerodynamic characteristics of interest of axially symmetric small launchers. The relation (5.4) has been developed for the body pressure drag coefficient estimation of blunted nose components. For the estimation of the normal force coefficient in compressible flow, the model (5.7) is developed. For the compressibility factor calculation, the polynomial approximation function (5.8) is suggested, its coefficients being presented in (5.9). Additionally, an extended CFD campaign was carried out, comprising of 72 cases, for the validation of the simplified mathematical model.
4. Development of two motion simulators necessary for the small launcher trajectory definition. The first uses a simplified dynamic model, with 3 degrees of freedom, having a total of 6 differential equations (detailed in subchapter 6.5.2), being further capable of optimizing the trajectory. The second simulator is based on a complex dynamic model, with 6 degrees of freedom, totaling a number of 21 differential equations (detailed in subchapter 6.5.1), being used to validate the reference trajectory.
5. Development of a multidisciplinary optimization algorithm for the preliminary design of small launcher configurations, having minimum lift-off mass, capable of successfully inserting a predefined payload in a target orbit, based on the algorithms developed in chapters 3-6 of the thesis. Using a hybrid solution selection and advancement algorithm, which initially uses a genetic algorithm followed by a gradient-based one (detailed in subchapter 7.1), along with the suggested objective function formulation (detailed in subchapter 7.4), the developed code generates both the constructive solution of the launcher, as well as the reference trajectory to be followed, respecting all the requirements and design restrictions imposed.
6. Optimization of a nominal small launcher constructive solution, capable of fulfilling a mission of current interest (insertion of a 130 kg satellite into a circular, polar orbit with an altitude of 400 km), according to the information presented in subchapter 8.3. The baseline trajectory of the launcher is defined (detailed in subchapter 8.4), ending with its validation (presented in subchapter 8.5).
7. Methodology for performing parametric analyzes on the impact of target orbit altitude (detailed in subchapter 9.1), payload mass (detailed in subchapter 9.2), typical missions (detailed in subchapter 9.3), and also used propellant type (detailed in subchapter 9.4) on the constructive solutions of small launchers. Generating a total of 20 space launchers for missions of interest.

10.2 Results obtained

The thesis summarizes a series of studies on the main aspects necessary for the preliminary design of small launchers constructive solutions. Based on these studies, individual computational codes were developed for sizing the launcher, to determine its propulsive and aerodynamic characteristics, together with simulating the dynamics of motion and optimizing the trajectory, which were validated using data from existing launchers, extracted from the literature. Finally, incorporating the previously validated codes, a multidisciplinary optimization algorithm (MDO) was developed capable of generating constructive solutions specific to small launchers. The constructive solutions generated with the developed algorithm are capable of fulfilling the imposed mission (to insert one or more satellites in a predefined orbit), the optimization being done by minimizing the lift-off mass of the launcher.

The first chapter presents the current global context of small launchers and the current state of research in the field. The second chapter details the work scheme implemented within the developed multidisciplinary optimization code.

The mathematical model used for sizing the small launcher, detailed in Chapter 3, is validated using 8 stages belonging to existing launchers or ones used in the past. The computational algorithm developed using this model estimates the structural mass of the liquid propellant stages with an average error of approximately 6.1% and their length with an average error of 5.4%. For a quick pre-sizing of the launcher, the accuracy of the results is sufficient.

The mathematical model used to determine the propulsive performance of small launchers, detailed in Chapter 4, is validated using 11 liquid propellant engines with different oxidizer-fuel pairs. The code developed using this model estimates the specific impulse and thrust generated with an average error of about 1.6%, being also very fast due to the implementation of the propulsive parameters approximation functions.

The mathematical model used to determine the aerodynamic characteristics of small launchers, detailed in Chapter 5, is validated using an extensive CFD campaign developed in the thesis. Based on the 72 CFD cases, performed with the help of the Ansys Fluent software package, a high-fidelity aerodynamic database was obtained. The computational code developed using simple analytical and semi-empirical models, estimates the aerodynamic coefficient of drag, lift, axial force and normal force with a high degree of accuracy.

The mathematical model used for launcher motion dynamics and trajectory optimization, detailed in Chapter 6, is a simplified 3DOF with zero roll-velocity angle, being selected due to its simplicity and high accuracy in modeling the motion of space vehicles. Following the comparisons between the data obtained with the computational code based on the model developed in the thesis and the reference data of the SpaceX Falcon 1 and Falcon 1e launchers, an average error of approximately 6.9% in payload mass inserted into orbit was observed. Of the 14 cases studied, the developed code generated a better trajectory (characterized by a higher payload mass inserted into orbit with the same launcher than the reference one) in 12 situations.

For the solution advancement in the iterative optimization process, represented by an optimization variables vector, a hybrid algorithm was used, based on a performance analysis of the genetic and gradient algorithms, presented in Chapter 7.

Chapter 8 detailed the nominal MDO case, being generated a launcher optimal constructive solution (from a minimum mass point of view) capable of inserting a payload mass of 130 kg into a circular, polar orbit of 400 km altitude with launch from Andøya Space Center, Norway. A launcher with a lift-off mass of 11.56 t, a total length of 17.64 m and an outer diameter of 1.35 m was obtained, the payload performance index being a high one for such a mission, of

1.12%. Also, an additional developed computational code (motion simulator) based on the 6DOF dynamic model was used to validate the reference trajectory generated by the MDO algorithm. A good correspondence was observed between the results, the motion around the center of mass being damped, thus there is no risk of destabilization of the launcher.

The objective of Chapter 9 was to present the influence of the main design requirements on the characteristics of the launcher. In subchapter 9.1 the impact of the target orbit altitude on the small launcher was studied, being analyzed 5 missions, with altitudes of the circular, polar, target orbit between 200 and 600 km, with an increment of 100 km. A quasi-linearity relationship was observed between the orbit altitude and the lift-off mass of the launcher, obtaining a minimum value for the 200 km altitude case (Lift-off mass = 9.92 t) and a maximum value in the case of a 600 km altitude orbit (Lift-off mass = 13.96 t).

In subchapter 9.2 the impact of the payload mass on the launcher was studied, being analyzed 9 missions, with payloads between 10 and 250 kg, with an increment of 30 kg. A quasi-linearity relationship was observed between the payload mass and the lift-off mass of the launcher, a sharp decrease in the payload performance index for low payload masses appearing. Values of payload performance index higher than 1% are observed for payloads of more than 100 kg.

In subchapter 9.3 the impact of the typical missions on the small launcher was studied, being analyzed 5 missions, with different launch locations and target orbit inclinations, specific to the approximately equatorial orbits, the International Space Station (ISS) orbit, the polar orbit, and also Sun-synchronous orbit (SSO). A significantly lower lift-off mass is observed at low orbit inclinations, launched from a location with similar latitude to the target orbit (Kourou and Omelek). The most penalizing orbit from launcher lift-off mass point of view is the SSO, having an inclination specific to the 400 km altitude of 97.03° , the lift-off mass being approximately 45% higher than in the case of an 5.3° inclination orbit. In addition, a comparison of the satellites Earth's coverage is presented, maximum coverage being seen for the polar orbit.

In subchapter 9.4 the impact of the propellant used on the small launcher was studied, being analyzed a total of 4 pairs of liquid propellants, having as oxidizer liquid oxygen and liquid fuel hydrogen (Launcher H-H), methane (Launcher M-M), kerosene (Launcher K-K) and ethanol (Launcher E-E). The target orbit was considered the circular, polar one of 400 km altitude, the payload mass being 130 kg. A very low lift-off mass is observed in the case of the H-H type launcher, due to its very high propulsive performances. The use of ethanol is not justified due to the very high lift-off mass associated. The simplicity of the technical solution required to use methane or kerosene as fuel (compared to hydrogen) justifies their use in the detriment of the optimal solution of the H-H launcher.

10.3 Prospects for future development

For further development it is envisioned the extension of the multidisciplinary optimization algorithm capabilities by modeling also solid propellant rocket engines, being necessary mathematical models capabilities related to the sizing and calculation of propulsive performance. Also of interest is the implementation of stages with a retropropulsion option for safe recovery and reusability. For the 6DOF motion simulator developed in the thesis, the extension of the existing capabilities is considered by including the elastic oscillation modes, specific to space launchers and the influence of wind on the trajectory.

10.4 List of publications

During the doctoral activities a total of 13 papers were published in international scientific journals, 7 articles as main author and 6 articles as co-author.

- As main author:

A. I. Onel, T. P. Afilipoae, A. M. Neculăescu, M. V. Pricop, “MDO approach for a two-stage microlauncher,” *INCAS Bulletin*, vol. 10, no. 3, pp. 127-138, 2018.

A. I. Onel, A. Stăvărescu, M. G. Cojocaru, M. V. Pricop, M. L. Niculescu, A. M. Neculăescu, T. P. Afilipoae, “Computation of the Hypersonic Heat Flux with Application to Small Launchers,” *AIP Conference Proceedings*, vol. 2046, 2018.

A. I. Onel, T. P. Afilipoae, A. M. Neculăescu, M. V. Pricop, “Drag coefficient modelling in the context of small launcher optimisation,” *INCAS Bulletin*, vol. 10, no. 4, pp. 103-116, 2018.

A. I. Onel, O. I. Popescu, A. M. Neculăescu, T. P. Afilipoae, T. V. Chelaru, “Liquid rocket engine performance assessment in the context of small launcher optimisation,” *INCAS Bulletin*, vol. 11, no. 3, pp. 135-145, 2019.

A. I. Onel, T. V. Chelaru, “Aerodynamic assessment of axisymmetric launchers in the context of multidisciplinary optimisation,” *INCAS Bulletin*, vol. 12, no. 1, pp. 135-144, 2020.

A. I. Onel, T. V. Chelaru, “Trajectory assessment and optimisation in the context of small launcher design,” *INCAS Bulletin*, vol. 12, no. 2, pp. 117-132, 2020.

A. I. Onel, T. V. Chelaru, “Weights and sizing assessment in the context of small launcher design,” *INCAS Bulletin*, vol. 12, no. 3, pp. 137-150, 2020.

- As co-author:

T. V. Chelaru, **A. I. Onel**, A. Chelaru, “Microlauncher, mathematical model for orbital Injection,” *International Journal Of Geology*, vol. 10, 2016.

T. V. Chelaru, **A. I. Onel**, T. P. Afilipoae, A. M. Neculăescu, “Mathematical Model for Microlauncher performances evaluation,” *UPB Scientific Bulletin, Series D: Mechanical Engineering*, vol. 79, no. 4, pp. 49-66, 2017.

T. P. Afilipoae, A. M. Neculăescu, **A. I. Onel**, M. V. Pricop, A. Marin, A. G. Perșinaru, A. M. Cișmilianu, I. C. Oncescu, A. Toader, A. Sirbi, S. Bennani, T. V. Chelaru, “Launch Vehicle - MDO in the development of a Microlauncher,” *Transportation Research Procedia*, vol. 29, pp. 1-11, 2018.

A. M. Neculăescu, T. P. Afilipoae, **A. I. Onel**, M. V. Pricop, I. Stroe, “Trajectory Optimization For Small Launchers Using A Genetic Algorithm Approach,” *AIP Conference Proceedings*, vol. 2046, 2018.

T. V. Chelaru, V. Pană, **A. I. Onel**, T. P. Afilipoae, A. F. Cojocaru, I. C. Vasile, “Flexible model for Micro-Launcher Dynamics,” *MATEC Web of Conferences*, vol. 304, 2019.

T. V. Chelaru, V. Pană, **A. I. Onel**, T. P. Afilipoae, A. F. Cojocaru, I. C. Vasile, “Wind Influence on Micro-Launcher Dynamics Model,” *MATEC Web of Conferences*, vol. 304, 2019.

Bibliography (selective)

- [1] F. Gamgami, "A trendsetting Micro-Launcher for Europe," in *3rd European Conference for Aeronautics and Space Sciences*, Versailles, 2009.
- [2] N. Brown, J. Olds, "Evaluation of Multidisciplinary Optimization (MDO) Techniques Applied to a Reusable Launch Vehicle," in *43rd AIAA Aerospace Sciences Meeting and Exhibit*, Reno, Nevada, USA, 2005.
- [3] M. Tava, S. Suzuki, "Integrated Multidisciplinary and Multicriteria Optimization of a Space Transportation System and its Trajectory," in *54th International Astronautical Congress of the International Astronautical Federation*, Bremen, Germany, 2003.
- [4] J. Martins, C. Marriage, "An Object-Oriented Framework for Multidisciplinary Design Optimization," in *3rd AIAA Multidisciplinary Design Optimization Specialist Conference*, Waikiki, Hawaii, USA, 2007.
- [5] I. Kroo, "Distributed multidisciplinary design and collaborative optimization," in *VKI lecture series on optimization methods and tools for multicriteria/multidisciplinary design*, 2004.
- [6] C. Gang, X. Min, W. Zi-Ming, C. Si-Lu, "Multidisciplinary design optimization of RLV reentry trajectory," in *13th International Space Planes and Hypersonic Systems and Technologies Conference*, Capua, Italy, 2005.
- [7] A. Filatyev, A. Golikov, "The complex approach to optimization of STS parameters on the maximum principle basis," in *59th International Astronautical Congress*, 2008.
- [8] S. Akhtar, H. Linshu, "Simulation-Based Optimization Strategy for Liquid Fueled Multi-stage Space Launch Vehicle," in *Sixth International Conference on Parallel and Distributed Computing, Applications and Technologies*, Dalian, China, 2005.
- [9] C. Geetha Krishnan, P. Mujumbar, K. Sudhakar, W. Adimurthy, "Genetic algorithm guided gradient search for launch vehicle trajectory optimization," in *International Conference on Aerospace Science and Technology*, Bangalore, India, 2008.
- [10] M. Balesdent, N. Bérend, P. Dépincé, A. Chriette, "A survey of multidisciplinary design optimization methods in launch vehicle design," *Structural and Multidisciplinary Optimization*, vol. 45, pp. 619-642, 2012.
- [11] F. Castellini, "Multidisciplinary design optimization for expendable launch vehicles," Politecnico Di Milano, 2012.
- [12] M. W. van Kesteren, B. T. C. Zandbergen, "Design and Analysis of an Airborne, Solid Propelled, Nanosatellite Launch Vehicle Using Multidisciplinary Design Optimization," in *6th European Conference For Aeronautics And Space Sciences (Eucass)*, Poland, 2015.
- [13] M. Balesdent, "Multidisciplinary Design Optimization of Launch Vehicles," Ecole Centrale de Nantes, 2011.
- [14] R. Humble, G. Henry, W. Larson, *Space Propulsion Analysis and Design*, Mc-Graw Hill, 1995.

- [15] *** Rocket & Space Technology, „Propellant Combustion Charts,” [Interactiv]. Available: <http://www.braeunig.us/space/comb.htm>.
- [16] J. J. Moré, D. C. Sorensen, "Computing a Trust Region Step," *SIAM Journal on Scientific and Statistical Computing*, vol. 3, pp. 553-572, 1983.
- [17] K. Levenberg, "A Method for the Solution of Certain Problems in Least Squares," *Quarterly of Applied Mathematics*, vol. 2, pp. 164-168, 1944.
- [18] J. N. Nielsen, Missile Aerodynamics, Mountain View, California, 1988.
- [19] *** United States Bureau of Naval Weapons, "Handbook of Supersonic Aerodynamics. Section 8. Bodies of Revolution," Navweeps Report 1488, 1961.
- [20] S. F. Hoerner, Fluid-Dynamic Drag, Published by the author, 1965.
- [21] W. Stoney, "Collection of Zero-Lift Drag Data on Bodies of Revolution from Free-Flight Investigations," NASA-TR-R-100, 1961.
- [22] C. S. James, R. C. Carros, "Experimental investigation of the zero-lift drag of a fin-stabilized body of fineness ratio 10 at Mach numbers between 0.6 and 10," NACA RM A53D02, Washington, 1953.
- [23] J. Barrowman, "The Practical Calculation of the Aerodynamic Characteristics of Slender Finned Vehicles," The Catholic University of America, Washington, 1967.
- [24] S. Box, C. M. Bishop, H. Hunt, "Estimating the dynamic and aerodynamic parameters of passively controlled high power rockets for flight simulation," 2009.
- [25] G. K. Mandell, G. J. Caporaso, W. P. Bengen, "Topics in Advanced Model Rocketry," MIT Press, 1973.
- [26] R. Galejs, "Wind Instability, What Barrowman Left Out," 1999.
- [27] F. Shahid, M. Hussain, M. M. Baig, I. Haq, "Variation in Aerodynamic Coefficients with Altitude," *Results in Physics*, vol. 7, pp. 1261-1273, 2017.
- [28] J. D. Gray, E. E. Lindsay, "Force Tests of Standard Hypervelocity Ballistic Models HB-1 and HB-2 at Mach 1.5 to 10," AEDC-TDR-63-137, 1963.
- [29] J. D. Gray, "Summary Report on Aerodynamic Characteristics of Standard Models HB-1 and HB-2," AEDC-TDR-64-137, 1964.
- [30] G. Pezzella, A. Viviani, Aerodynamic and Aerothermodynamic Analysis of Space Mission Vehicles, Springer, 2015.
- [31] T. V. Chelaru, C. Mihăilescu, Lansatoare și sisteme de lansare - Note de curs, București: Politehnica Press, 2017.
- [32] A. A. Lebedev, N. F. Gerasiota, Balistika raket, Moskva: Ed. Maşinostroenie, 1970.
- [33] *** SpaceX, "Falcon 1 Launch Vehicle Payload Users's Guide, Rev.7," 2008.